PROJECT ADMINISTRATION DATA SHEET

[X] ORIGINAL [ ] REVISION NO. ______

Project No. A-3675 GTRI/~~GIT~~ DATE 10 / 04 / 83

Project Director: John Gilmore ~~School~~/Lab EML

Sponsor: Martin Marietta

Type Agreement: Purchase Agreement No. ZD/958162

Award Period: From 9/19/83 To ~~12/16/83~~ 1/15/84 (Performance) ______ (Reports)

Sponsor Amount: This Change Total to Date

Estimated: $ ______ $ ______

Funded: $ 4,000 $ 4,000

Cost Sharing Amount: $ ______ Cost Sharing No: ______

Title: "Obstacle Avoidance Conceptual Design"

ADMINISTRATIVE DATA OCA Contact Frank Huff X4820

1) Sponsor Technical Contact:

Martin Marietta
P. O. Box 5837
Orlando, FL 32855
Attn: Wade Pemberton

(305) 352-3308

2) Sponsor Admin/Contractual Matters:

Martin Marietta
P. O. Box 5837
Orlando, FL 32855
Attn: R. W. Conrad
Mail No. 539
(305) 352-3308

Defense Priority Rating: None

Military Security Classification: ______
(or) Company/Industrial Proprietary: N/A

RESTRICTIONS

See Attached ______ Supplemental Information Sheet for Additional Requirements.

Travel: Foreign travel must have prior approval — Contact OCA in each case. Domestic travel requires sponsor approval where total will exceed greater of $500 or 125% of approved proposal budget category.

Equipment: Title vests with N/A; none proposed.

COMMENTS:

OCT 1983
RECEIVED
Research Reports
Office

COPIES TO:

Project Director
Research Administrative Network
Research Property Management
Accounting

Procurement/EES Supply Services
Research Security Services
Reports Coordinator (OCA)
Research Communications (2)

GTRI
Library
Project File
Other Newton

FORM OCA 4:383

GEORGIA INSTITUTE OF TECHNOLOGY   OFFICE OF CONTRACT ADMINISTRATION

SPONSORED PROJECT TERMINATION/CLOSEOUT SHEET

Date February 14, 1984

Project No. A-3675   ~~School~~/Lab EML

Includes Subproject No.(s) ----

Project Director(s) John Gilmore   GTRI / ~~GIT~~

Sponsor Martin Marietta

Title "Obstacle Avoidance Conceptual Design"

Effective Completion Date: 1/15/84 (Performance) 1/15/84 (Reports)

Grant/Contract Closeout Actions Remaining:

- [ ] None
- [x] Final Invoice ~~or Final Fiscal Report~~
- [ ] Closing Documents
- [ ] Final Report of Inventions
- [ ] Govt. Property Inventory & Related Certificate
- [ ] Classified Material Certificate
- [ ] Other ______

Continues Project No. ______   Continued by Project No. ______

COPIES TO:

Project Director
Research Administrative Network
Research Property Management
Accounting
Procurement/EES Supply Services
Research Security Services
Reports Coordinator (OCA)
Legal Services

Library
GTRI
Research Communications (2)
Project File
Other ______

Form OCA 60:1028

FINAL REPORT

OBSTACLE AVOIDANCE CONCEPTUAL DESIGN

By
John F. Gilmore

Prepared for
MARTIN MARIETTA
ORLANDO, FLORIDA

Under
Purchase Agreement No. ZD/958162

Report Period 19 September 83 – 15 January 84

JANUARY 1984

GEORGIA INSTITUTE OF TECHNOLOGY
A Unit of the University System of Georgia
Engineering Experiment Station
Atlanta, Georgia 30332

1984

FINAL REPORT

OBSTACLE AVOIDANCE CONCEPTUAL DESIGN

By

JOHN F. GILMORE

Under

Purchase Agreement No. ZD/958162

Prepared for

MARTIN MARIETTA
ORLANDO, FLORIDA

Report Period 9/19/83 – 1/15/84

JANUARY 1984

Obstacle Avoidance Conceptual Design

1.0 This is the first of three status reports dealing with the development of an obstacle avoidance algorithm for tower detection. The objective of this work is to design an algorithm capable of detecting one meter wide towers from ranges greater than 1.5 kilometers. The sensor used is assumed to have a height of 61 meters (± 15%) while the towers to be detected will also be approximately 61 meters (± 15%) tall. The objectives of this report are as follows:

(1) Survey literature on tower detection algorithms.

(2) Critique existing algorithms in terms of applicability to the MUFFLIR scenario.

(3) Describe a system approach to tower detection flexible enough to handle various types of imagery (FLIR, video, synthetic).

(4) Create a synthetic database for initial testing.

(5) Outline the research being performed for the next status report.

2.0 Tower Detection Literature Search

A literature search was performed in an attempt to identify previous work in the area of tower detection. A total of twelve references [Appendix A] were generated, but they related mostly to applications dealing with radar. The search was further broadened to cover collision and terrain avoidance. This generated seven additional references [Appendix B] that were of interest to the overall MUFFIR scenario but not of direct application.

In terms of an algorithm for detecting towers at low flying altitudes, the lack of previous work indicates that the effort underway is:

(1) state-of-the-art as no other activities in this area can be identified, and

(2) probably very difficult in nature as most of the simple detection problems have been solved and published by the academic (and partly by the aerospace) community.

3.0 System Approach

In order to accurately detect towers in visual imagery, their limited characteristics must be fully exploited. A priori tower information in the MUFFLIR scenario includes the following facts:

(1) The towers will be 61 meters (± 15%) in height and one meter in width.

(2) The sensor will be flying at approximately 61 meters (± 15%) and will therefore always be within 18 meters of the tower height.

(3) The tower must be detected at sufficient range to permit the aircraft to automatically avoid the tower without pilot intervention and

without the aircraft being required to sustain more than 1g. This range is projected to be approximately 1.5 kilometers.

(4) The tower will be $1^{o}C$ above ambient air temperature.

(5) The Imagery used is assumed to be heads-up, therefore towers will be vertical with respect to the horizon.

Two locations exist in which towers may occur: open fields and forest areas. Based on this, two hypothesis were initially made during algorithm design. The first is that a vertical tower in a horizontal field may produce an inverted "T" effect which should be detectable. The second is that typically two-thirds of the tower will extend above the forest area. The fact that tree top regions are rather busy with edges also provides some contextual information in regards to the inverted "T" horizon base.

Based upon this information, a proposed tower detection system was created as shown in Figure 1. The system consists of four major stages preprocessing, edge detection, prescreening and structural analysis.

Preprocessing consists of enhancing the edge quality of the image as well as removing the random noise produced in most sensors. As synthetic imagery is rather noise free and crisp, the first phase of this task doesn't make use of the enhancement techniques that are required for video and infrared image. When video data is received from Martin Marietta's Simulation and Test Lab, a decision will be made on applicable enhancement techniques based image quality. The

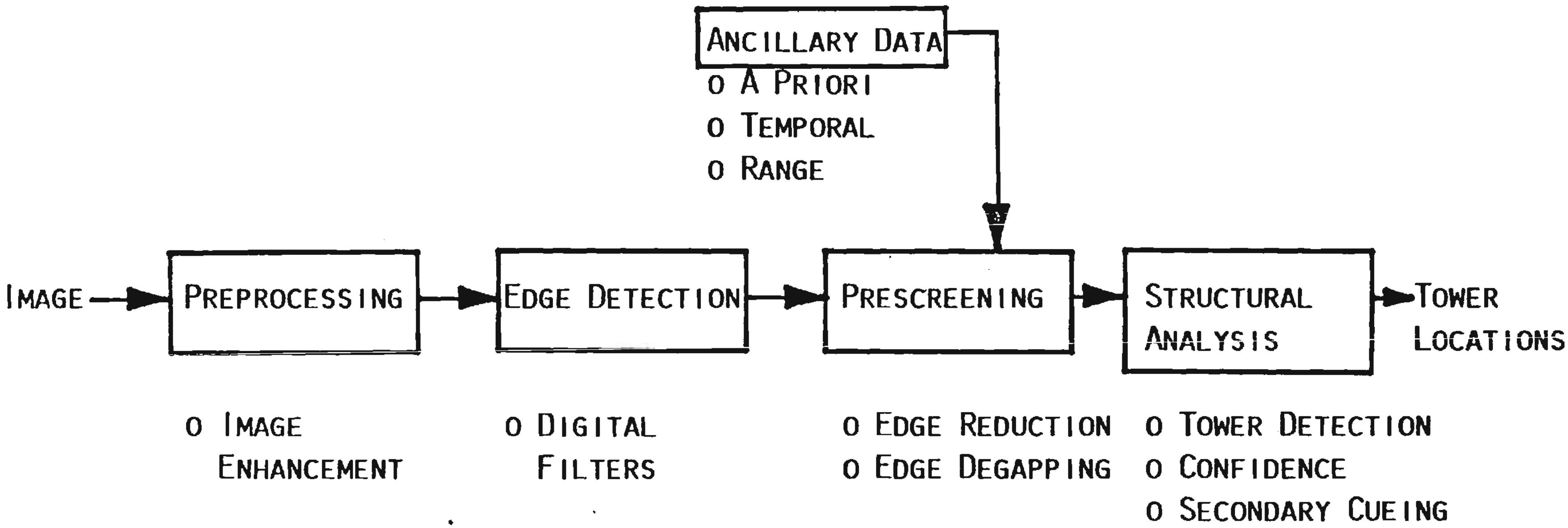

FIGURE 1. TOWER DETECTION SYSTEM

preprocessing performed will always be determined by the type of imagery provided therefore requiring multiple enhancement techniques to exist within the system.

Edge detection convolves a number of digital filters with the image in an attempt to identify the location of strong object and region edges. As with preprocessing, each type of imagery will require different types of filters. Twelve different types of edge filters exist are in current system. They are

- Roberts	- Argyle
- Sobel	- Macleod
- Compass Gradient	- Frei-Chen
- Kirsch	- Prewitt
- Laplacian	- Energy
- Magnitude Contrast	- Star

The extraction of lines that correspond to objector region edges is based on the assumption that the light intensity is constant or smoothly varying over the image of an object face and jumps discontinuously at the intersection with the image of another face. This assumption is valid if the object surfaces are smooth, homogeneous, and opaque and the lighting is uniform and arranged to eliminate shadows.

In a continuous image plane, points at which the intensity changes discontinuously are easily identified to be those where the gradient of the intensity function is either infinite or larger than a predetermined threshold. An approximation for this gradient for a digital picture is given by

$$R(i,j) = \sqrt{\{g(i+1,j+1)-g(i,j)\}^2+\{g(i,j+1)-g(i+1,j)\}^2}$$

where g(i,j) is the image intensity at pixel (i,j) (Figure 2).

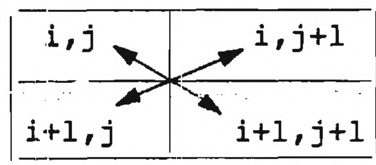

Figure 2. Robert's Gradient Operator

The direction of the gradient is then given by the angle α, where

$$\alpha = -\frac{\pi}{4} + \tan^{-1}\left[\frac{g(i,j+1)-g(i+1,j)}{g(i+1,j+1)-g(i,j)}\right]$$

The above definition of gradient is called the Robert's Cross Operator [1]. An edge is said to be present at pixel (i,j) if R(i,j) is less than a chosen threshold.

Due to its size, the Robert Cross Operator is not immune to the effects of noise. For this reason, the use of a larger neighborhood, such as the 3-by-3 Sobel [2] operator, typically produces more reliable results. The Sobel operator (Figure 3) basically forms a nonlinear computation of the edge magnitude for a given pixel.

1	2	1
0	0	0
-1	-2	-1

1	0	-1
2	0	-2
1	0	-1

Figure 3. Horizontal & Vertical Sobel Operators

Compass Gradient [3] Masks (Figure 4) convolve with an image array to produce a two-dimensional discrete differentiation, but as with the Sobel operator, require a mask for each different edge direction being analyzed. Additionally, gradient masks use zero weighting so that there is no output response over constant luminance regions of an image. Kirsch [4] has used an edge detector with slightly different masks (Figure 5) which employ a non-zero weighting scheme. Again eight masks are used in order to determine direction.

1	1	1
1	-2	1
-1	-1	-1

1	1	1
-1	-2	1
-1	-1	1

-1	1	1
-1	-2	1
-1	1	1

-1	-1	1
-1	-2	1
1	1	1

-1	-1	-1
1	-2	1
1	1	1

-1	-1	-1
1	-2	1
1	1	1

1	-1	-1
1	-2	-1
1	1	1

1	1	-1
1	-2	-1
1	1	-1

1	1	1
1	-2	-1
1	-1	-1

Figure 4. Compass Gradient Masks

Edge sharpening, without regard to edge direction, can be obtained by convolution of an image with a Laplacian mask [5]. Several types of Laplacian masks are shown in Figure 6.

KIRSCH

$$\begin{bmatrix} 5 & 5 & 5 \\ -3 & \emptyset & -3 \\ -3 & -3 & -3 \end{bmatrix} \quad \begin{bmatrix} -3 & 5 & 5 \\ -3 & \emptyset & 5 \\ -3 & -3 & -3 \end{bmatrix} \quad \begin{bmatrix} 5 & -3 & -3 \\ 5 & \emptyset & -3 \\ 5 & -3 & -3 \end{bmatrix} \quad \begin{bmatrix} -3 & -3 & -3 \\ -3 & \emptyset & 5 \\ -3 & 5 & 5 \end{bmatrix}$$

$$\begin{bmatrix} -3 & -3 & -3 \\ -3 & \emptyset & -3 \\ 5 & 5 & 5 \end{bmatrix} \quad \begin{bmatrix} -3 & -3 & -3 \\ 5 & \emptyset & -3 \\ 5 & 5 & -3 \end{bmatrix} \quad \begin{bmatrix} 5 & -3 & -3 \\ 5 & \emptyset & -3 \\ 5 & -3 & -3 \end{bmatrix} \quad \begin{bmatrix} 5 & 5 & -3 \\ 5 & \emptyset & -3 \\ -3 & -3 & -3 \end{bmatrix}$$

FIGURE 5. KIRSCH FILTERS

0	-1	0
-1	4	-1
0	-1	0

-1	-1	-1
-1	8	-1
-1	-1	-1

1	-2	1
-2	4	-2
1	-2	1

Figure 6. Laplacian Masks

The magnitude contrast algorithm [6] exploits the luminance contrast of edge regions to extract edge elements without regard to direction. Arglye [7] and Macleod [8] operators (Figure 7) make use of gaussian-shaped weighting functions. In these masks, the edge weights drop exponentially as the distance from the edge increases. The weights also drop along the edge as the distance from the center increases. Gaussian masks basically de-emphasize the effects of points away from the center.

Frei and Chen [9] have developed eight orthogonal vectors that form a complete basis (Figure 8). The first four masks are suitable for the detection of edges whereas the last four masks represent templates suitable for line detection.

The Prewitt filters [2] are similar to the Kirsch operators but are based on a different non-zero weighting scheme weighting as shown in Figure 9. The energy filters were designed by Laws [9] to extract texture patterns for region classification. Only five of the original dozen are used in this work as they specifically relate to edges extraction (Figure 10). The Star [10] filter (also shown in Figure 10) is an operator based on this same theme.

GAUSSIAN-SHAPED WEIGHTING FUNCTIONS

[1] ARGYLE FUNCTION - A SPLIT GAUSSIAN FUNCTION DEFINED IN ONE DIMENSION AS

$$H(X) = EXP \left\{ -1/2 \left(\frac{X}{P}\right)^2 \right\} \text{ FOR } X \geq 0$$

$$H(X) = -EXP \left\{ -1/2 \left(\frac{X}{P}\right)^2 \right\} \text{ FOR } X < 0$$

WHERE P IS A SPREAD FUNCTION

[2] MACLEOD FUNCTION - SUPPRESSES THE EFFECT OF PIXEL VALUES IN THE EDGE TRANSITION REGION

$$H(X) = EXP \left\{ -1/2 \left(\frac{Y}{T}\right)^2 \right\} \left[EXP \left\{ -1/2 \left(\frac{X-P}{P}\right)^2 \right\} - EXP \left\{ -1/2 \left(\frac{X+P}{P}\right)^2 \right\} \right]$$

WHERE P AND T ARE SPREAD FUNCTIONS

FIGURE 7. ARGYLE AND MACLEOD FUNCTIONS

FREI AND CHEN

$$\begin{bmatrix} 1 & \sqrt{2} & 1 \\ 0 & 0 & 0 \\ -1 & -\sqrt{2} & -1 \end{bmatrix} \quad \begin{bmatrix} 1 & 0 & -1 \\ \sqrt{2} & 0 & -\sqrt{2} \\ 1 & 0 & -1 \end{bmatrix} \quad \begin{bmatrix} 0 & -1 & \sqrt{2} \\ 1 & 0 & -1 \\ -\sqrt{2} & 1 & 0 \end{bmatrix} \quad \begin{bmatrix} \sqrt{2} & -1 & 0 \\ -1 & 0 & 1 \\ 0 & 1 & -\sqrt{2} \end{bmatrix}$$

BASIS OF EDGE SUBSPACE

$$\begin{bmatrix} 0 & 1 & 0 \\ -1 & 0 & -1 \\ 0 & 1 & 0 \end{bmatrix} \quad \begin{bmatrix} -1 & 0 & 1 \\ 0 & 0 & 0 \\ 1 & 0 & -1 \end{bmatrix} \quad \begin{bmatrix} 1 & -2 & 1 \\ -2 & 4 & -2 \\ 1 & -2 & 1 \end{bmatrix} \quad \begin{bmatrix} -2 & 1 & -2 \\ 1 & 4 & 1 \\ -2 & 1 & -2 \end{bmatrix}$$

BASIS OF LINE SUBSPACE

FIGURE 8. FREI AND CHEN ORTHOGONAL VECTORS

1	1	-1
1	-2	-1
1	1	-1

1	-1	-1
1	-2	-1
1	1	1

Figure 9. Prewitt Operators

Once edges are detected, a prescreening occurs which consists of edge degapping and edge reduction. Due to the nature of digital imagery, contiguous edges may appear as line segments separated by pixel gaps. Edge degapping analyzes line segment continuity and fills localized gaps in an attempt to construct complete edges. The degapping process is limited to one and two pixel gaps due to the forward view of the sensor. Without this limitation natural terrain areas may appear as streaks due to the number of stray lines present. Edge reduction removes any remaining stray edges based upon size and edge strength.

Ancillary information in the form of temporal image history, range data, or any available a priori information is used during prescreening to aid in the detection of towers. This information indentifies high confidence areas and edge in the current image that should be maintained and exploited during prescreening.

Structural analysis performs the actual detection of towers and associates a detection confidence with each tower. Several convictions currently exist including the following:

0 Different edge detectors will be required for each type of imagery (e.g. synthetic, video, FLIR, etc.)

ENERGY FILTERS

EDGE (V)

-1	-2	0	2	1
-4	-8	0	8	4
-6	-12	0	12	6
-4	-8	0	8	4
-1	-2	0	2	1

EDGE

-1	0	2	0	-1
-4	0	8	0	-4
-6	0	12	0	-6
-4	0	8	0	-4
-1	0	2	0	-1

WAVE

-1	0	2	0	-1
-2	0	4	0	-2
0	0	0	0	0
2	0	-4	0	2
1	0	-2	0	1

SPOT

1	0	-2	0	1
0	0	0	0	0
-2	0	4	0	-2
0	0	0	0	0
1	0	-2	0	1

EDGE (H)

-1	-1	-1	-1	-1
-2	-2	-2	-2	-2
0	0	0	0	0
2	2	2	2	2
1	1	1	1	1

STAR

2	-4	1	-4	2
-4	2	1	2	-4
1	1	8	1	1
-4	2	1	2	-4
2	-4	1	-4	2

FIGURE 10. ENERGY AND STAR FILTERS

- Synthetic imagery is too ideal
- STL imagery is more representative of actual data

0 Temporal information will increase algorithm performance
- increased P_D, decreased F_A

0 Tower structure is a function of range
- Algorithms may need to be adaptive based on range
- Guide wires and substructure may be detectable at close range

0 A Knowledge-based approach may help avoid other threats
- Communication power line towers are usually linear in placement
- Wires may exist between towers or as supports

Figure 11 outlines the basic algorithm concept currently being developed on this task. The next status report will detail the specific algorithms being implemented as well as present results achieved using synthetic imagery.

5.0 Synthetic Database For Tower Detection

A synthetic database has been created for initial algorithm evaluation using the Georgia Tech Visual Model

BASIC ALGORITHM CONCEPT

1) DETECT ALL OF THE EDGES WITHIN AN IMAGE

2) DEGAP ADJACENT EDGES AND SUPRESS NOISY EDGES

3) LOCATE VERTICAL STRUCTURES

4) EXPLOIT NONVERTICAL EDGES FOR TERRAIN INFORMATION

5) PERFORM A TEMPORAL CORRESPONDENCE OF PAST FRAMES

6) EVALUATE HIGH PROBABILITY STRUCTURES

7) IDENTIFY TOWER LOCATIONS AND COMPUTE DETECTION CONFIDENCES

FIGURE 11. BASIC ALGORITHM CONCEPT

described in Appendix C. Using a DMA ARTBASS database (in which a pixel represents 12.5 with height tolerance of ± 1 meter), towers with a height of 61 meters (± 15%) are generated and correctly scaled to the topography in which they will be placed.

In the ARTBASS data itself, each facet contains a class number which is used to generate an accurate intensity model based upon the region types encountered. In this manner, an actual image of forests, river, roads, etc, is constructed and the tower model generated is then placed in an appropriate location. Any possible obscurations of the tower are accounted for creating a representative "tower" image which is placed in the database. The current database consists of several synthetic images of a tower in an open field and in a forest area with ranges varying from 2.0 to 0.5 kilometers. Appendix D contains a sample tower closure sequence as well as two distant views of the imagery created by the visual model. Initial algorithm evaluation using this imagery will occur during the second phase of this task.

6.0 Future Plans

The second phase of this activity consists of the following goals:

- 0 Complete work on the structural analysis component of the tower detection system
- 0 Create an ancillary information source for the existing synthetic database.
- 0 Detail and evaluate the end-to-end simulation (specifically the structural analysis algorithms) using the synthetic database

0 Acquire the Martin Marietta STL database to be used in actual algorithm performance analysis

Phase three of this task will concentrate on evaluating the tower detection system using STL data which will be more representative of actual system performance. Figure 12 outlines the entire project schedule from start to final report. At this time it is anticipated that several milestones will be met before scheduled allowing for further analysis of the simulation on FLIR data if available.

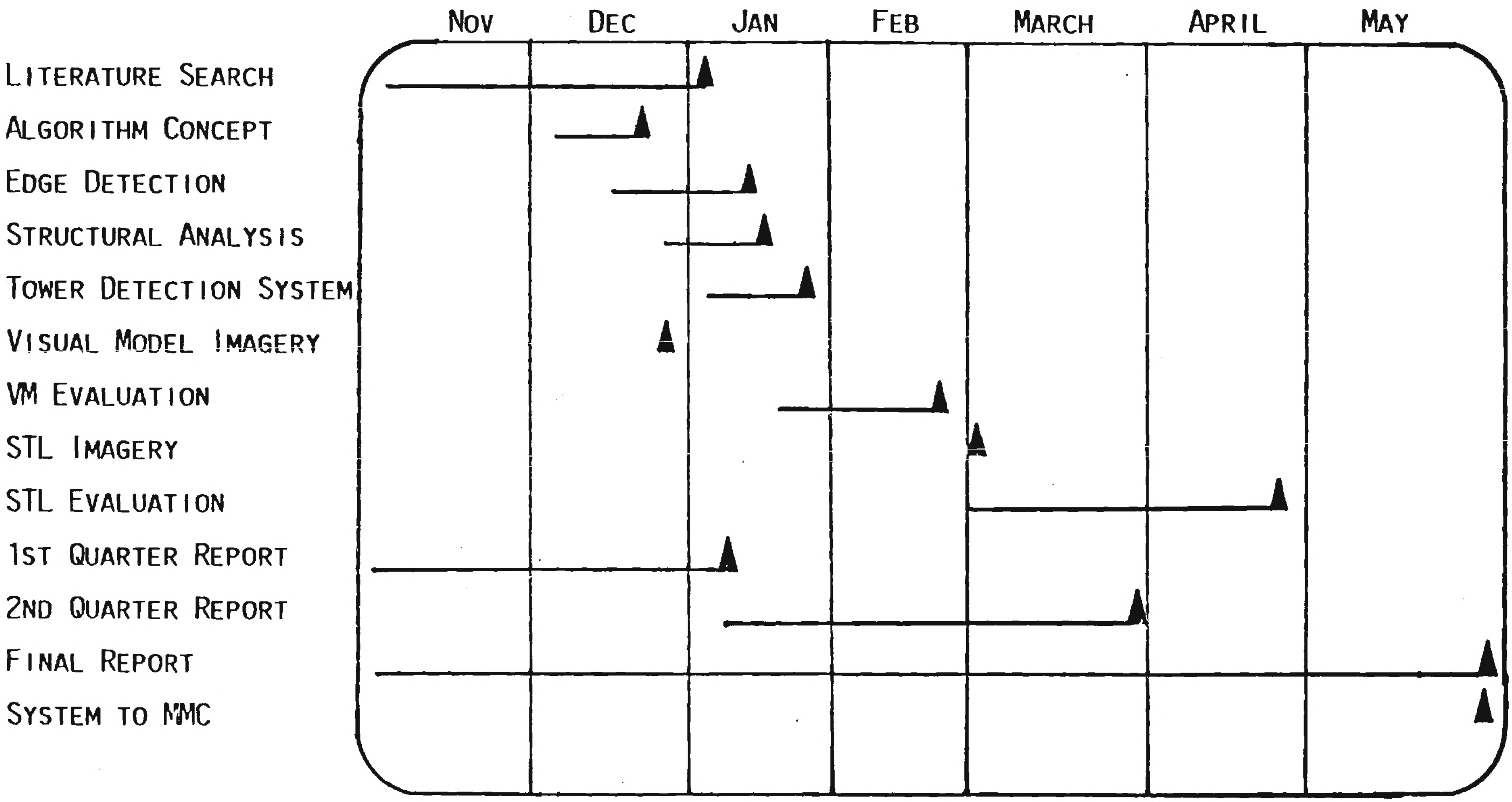

FIGURE 12. TOWER DETECTION MILESTONES

BIBLIOGRAPHY

[1] L. G. Roberts
"Machine Perception of Three-Dimensional Solids"
Optical and Electro-Optical Information Processing
MIT Press, Cambridge, Ma, 1968.

[2] J. M. S. Prewitt
"Object Enhancement and Extraction"
Picture Processing and Psychopictorics
Academic Press, New York, 1970

[3] W. K. Pratt
Digital Image Processing
John Wiley Press, New York, 1978

[4] R. A. Kirsch
"Computer Determination of the Constituent Structure of Biological Images"
Computers and Biomedical Research
Volume 4, No. 3, June 1971

[5] D. Marr and E. Hildreth
"Theory of Edge Detection
Proceedings of the Royal Society of London
B207, 1980

[6] J. F. Gilmore
"A Differentiation Based on Magnitude Contrast Segmentation Algorithm"
Proceedings of Digital Image Processing
SPIE, May 1981

[7] E. Argyle
"Techniques For Edge Detection"
Proceedings of IEEE, Feb. 1977

[8] I. D. G. Macleod
"On Finding Structure in Pictures"
Picture Language Machines
Academic Press, New York, 1970

[9] K. I. Laws
"Textured Image Segmentation"
Report 940, USC, Jan 1980

[10] P. J. Rowland
Context Cueing Techniques
Third Quarterly Report
July 1983

APPENDIX A. TOWER DETECTION

AD-C026 699   17/9   16/2   17/4

MASSACHUSETTS INST OF TECH LEXINGTON LINCOLN LAB

An Assessment of Look-Ahead Millimeter Wave Radars for Obstacle Detection. (U)

DESCRIPTIVE NOTE: Project rept.,
OCT 81   211P   Jao,Jen K. ;
REPT. NO. CMT-17
CONTRACT: F19628-80-C-0002, ARPA Order-3724
MONITOR: ESD,SBI   TR-81-281,AD-E500 461

SECRET REPORT
DECL-   OADR

ABSTRACT: This report assesses the feasibility of using active millimeter wave radars as obstacle detection and avoidance sensors for low-flying vehicles. The primary obstacle of interest is high-voltage power transmission lines. The analyses unveil several critical issues associated with power line detection requirements, including: radar sensitivity, range, and search angle; detection strategies; and sensor vulnerability to interception. The results quantify radar performance and design trade-offs in terms of power line geometry, radar cross section characteristics, current millimeter wave component technology, and effects of propagation, weather, and clutter. (U)

DESCRIPTORS: *Radar cross sections, *Guided missile trajectories, *Radar equipment, Millimeter waves, Forward looking infrared systems, Cruise missiles, Terrain avoidance, Terrain following, High voltage, Transmission lines, Detectors, Vulnerability, Interception, Propagation, Weather, Clutter, Sensitivity, Electric power, Low altitude, Radar clutter, Strategic weapons (U)

IDENTIFIERS: Obstacle detection, Tower detection, Forward looking radar (U)

UNCLASSIFIED

DTIC REPORT BIBLIOGRAPHY   SEARCH CONTROL NO. LTK53D

AD-C016 075L   17/5   17/8   15/4

MANTECH OF NEW JERSEY CORP ROCKVILLE MD

Area-Denial Munitions Detection Systems. (U)

DESCRIPTIVE NOTE: Final rept. 28 Mar-11 Nov 77,
SEP 78   160P   Plotkin,Neal ;Kresky,John ;
Karmarkar,Subhash ;Thompson,Thomas ;
CONTRACT: N00174-77-C-0182
MONITOR: NAVEODFAC   TR-193

CONFIDENTIAL REPORT
DECL-   31 Dec 93
Distribution limited to U.S. Gov't. agencies only; Test and Evaluation; Nov 77. Other requests for this document must be referred to Commanding Officer, Naval Explosive Ordnance Disposal Facility, Attn: 012A-Scty. Off. Indian Head, MD 20640.

DESCRIPTORS: *Ordnance locators, *Forward looking infrared systems, Optical detectors, Airborne, Landing fields, Area denial, Target signatures, Optical signatures, Infrared signatures, Aerial reconnaissance, Target recognition, Helicopters, Deployment, Photographic reconnaissance (U)

AD-A112 663 17/9 4/2

FEDERAL AVIATION ADMINISTRATION TECHNICAL CENTER ATLANTIC CITY NJ

Test and Evaluation of the Airport Radar Wind Shear Detection System. (U)

DESCRIPTIVE NOTE: Final rept. Mar 78-May 81,
FEB 82 39P Offi,Dominick L. ;Lewis, William ;Lee,Tai ;DeLaMarche,Alfred ;
REPT. NO. DOT-FAA-CT-81-63
MONITOR: FAA/RD 81/85

UNCLASSIFIED REPORT

ABSTRACT: A wind shear detection system, developed by the Wave Propagation Laboratory (WPL) to operate with the Federal Aviation Administration (FAA) Airport Surveillance Radar ASR-(8), was installed and tested at the FAA Technical Center. Initial tests consisted of hardware and software shakedown and feasibility determinations. Second phase tests compared radar with aircraft and tower winds, evaluated the wind shear measurement capability under various weather conditions, and investigated the effectiveness of a simple two-azimuth pointing strategy. Final efforts consisted of observations in all-weather regimes and tests of a modified velocity-azimuth display (VAD) and a glide slope scan. Results showed the system to be compatible with and to operate satisfactorily with the ASR-8. The processing and spectral display of clear air and precipitation returns is feasible. The accuracy of agreement between radar-measured winds and components of the aircraft-measured winds in both radially oriented flights and runway offset flights using a two-azimuth pointing technique, a glide slope scan, and a modified VAD was examined. Radar versus tower wind agreement was also examined. Potentially dangerous wind shears associated with weather during these tests were detectable. Certain system limitations were also defined and considered. (Author) (U)

DESCRIPTORS: *Meteorological radar, *Wind shear, *Search radar, *Doppler radar, Test and evaluation, Computer programs, Wind velocity, Wave propagation, Weather, Limitations, Measurement, Precipitation, Towers, Accuracy, Aircraft, Wind, Agreements, Radar, Air (U)

IDENTIFIERS: ASR(Airport Surveillance (U)

UNCLASSIFIED

DTIC REPORT BIBLIOGRAPHY SEARCH CONTROL NO. LTK53D

AD-A099 513 17/9

TRANSPORTATION SYSTEMS CENTER CAMBRIDGE MA

Detection Performance Evaluation of the ASDE-3 Using Fixed Frequency and Frequency-Agile Operation. (U)

DESCRIPTIVE NOTE: Final rept. Jan-Apr 80,
MAR 81 102P Bloom,P. J. ;Bishop,G. J. ;Kuhn,J. E. ;
REPT. NO. TSC-FAA-81-8
MONITOR: FAA-RD 81-41

UNCLASSIFIED REPORT

ABSTRACT: The ASDE-3 (Airport Surface Detection Equipment) Radar design has many features to enhance operational usefulness. The purpose of all these features is to provide a better airport surface surveillance display for the control power tower cab. One of these features is the use of frequency agility, the transmission at a different frequency within a frequency band during each radar transmit time. The function of this feature is to improve the detection performance of the ASDE radar and thereby improve the quality of the information presented on the operational display. The use of frequency agility reduces image breakup of aircraft on the display and, in rainy weather, allows the display of ground traffic during much heavier precipitation than achievable with fixed frequency operation. This report discusses the role of the ASDE in airport surface traffic control, and the theory of frequency agility benefits, and gives the empirical results obtained during field experiments using the ASDE-3 engineering model test bed. (U)

DESCRIPTORS: *Frequency agility, *Airport radar systems, Ground traffic, Radar images, Field tests, Performance(Engineering), Rain, Aircraft, Operation, Detection, Towers, Frequency, Precipitation, Surfaces, Power, Detectors, Control, Behavior, Airports, Benefits (U)

IDENTIFIERS: ASDE(Airport Surface Detection Equipment) (U)

AD- 885 321 4/1 1/1 1/2

BATTELLE-NORTHWEST RICHLAND WASH PACIFIC NORTHWEST LAB

Take-Off and Landing Critical Atmospheric Turbulence (TOLCAT) Experimental Investigation. (U)

DESCRIPTIVE NOTE: Interim rept. Mar 68-Nov 69,
MAY 71 342P Elderkin,C. E. ;Powell,D. C. ;Dunbar,A. G. ;Horst,T. W. ;
CONTRACT: F33615-68-M-5009
PROJ: AF-ADP682E
MONITOR: AFFDL TR-70-117

UNCLASSIFIED REPORT

ABSTRACT: A preliminary system for measuring, recording, and digitizing turbulence data was established and methods for data reduction and analyses were developed to describe the spatial and temporal aspects of turbulence. The system included a variety of sensors for evaluation, from which two were selected to be used in the final expanded measurement array. These two are the sonic and three-propeller anemometers. Computer programs were written for data reduction, moment, and probability distribution analyses, and for power spectral and cross spectral analyses. Turbulence data, from as many as seven simultaneously operated three-wind-component sensors mounted on towers, were collected in three different instrument arrays. The data were utilized to evaluate the multi-instrument operation for TOLCAT measurements, identifying necessary modifications that must be made to the instruments, their mounting supports, and procedures for calibration and operation. The data, recorded in the field on analog magnetic tape, were also utilized for establishing computer-controlled digitizing and digital data logging techniques. (Author) (U)
DESCRIPTORS: (*ATMOSPHERIC MOTION, MEASUREMENT), (*AIRCRAFT LANDINGS, ATMOSPHERIC MOTION), TAKEOFF, TURBULENCE, DETECTORS, METEOROLOGICAL INSTRUMENTS, TOWERS, ANEMOMETERS, MICROMETEOROLOGY, DIGITAL SYSTEMS, SHORT TAKEOFF AIRCRAFT, DATA PROCESSING (U)
IDENTIFIERS: ATMOSPHERES, BOUNDARY LAYER, *TAKEOFF AND LANDING CRITICAL ATMOSPHERIC TURBULENCE, *TOLCAT(TAKEOFF AND LANDING CRITICAL ATMOSPHERIC TURB(U)

UNCLASSIFIED

DTIC REPORT BIBLIOGRAPHY SEARCH CONTROL NO. LTK53D

AD- 842 698L 17/9 4/2

GOVERNMENTAL AFFAIRS INST WASHINGTON D C RESEARCH DIV

Mobile Weather Radar Set, AN/TPS-41 (XE-2). (U)

DESCRIPTIVE NOTE: Interim rept.
SEP 68 11P
CONTRACT: DAAG39-69-C-0001
PROJ: DA-1-H-664705-D-511
TASK: 1-H-664705-D-51102
MONITOR: AMC TIR-9.3.2.2(2)

UNCLASSIFIED REPORT

Distribution: DoD only: others to Commanding General, Army Electronics Command, Attn: AMSEL-BL. Fort Monmouth, N. J. 07703.
SUPPLEMENTARY NOTE: Supersedes Rept. no. TIR-9.3.2.2(1) dated Mar 68, AD-831 966L.

DESCRIPTORS: (*METEOROLOGICAL RADAR, MOBILE), WEATHER, RADAR ANTENNAS, NUCLEAR RADIATION, NUCLEAR WARFARE, SHELTERS, CATHODE RAY TUBES, PLAN POSITION INDICATORS, ANTENNA MASTS, NUCLEAR EXPLOSIONS, FALLOUT, ARMY EQUIPMENT, DATA, TOWERS, DETECTION, DRONES, IMAGES, ILLUMINATION, X BAND, DETONATIONS (U)
IDENTIFIERS: *AN/TPS-41, NUCLEAR CLOUDS, RANGE HEIGHT INDICATORS (U)

AD- 762 911 4/2 13/13

AIR FORCE CAMBRIDGE RESEARCH LABS L G HANSCOM FIELD MASS

An Annotated Listing-Tall Towers Instrumented for Wind Observations. (U)

DESCRIPTIVE NOTE: Air Force surveys in geophysics,
MAR 73 24P Cormier,Rene F. ;
REPT. NO. AFCRL-TR-73-0179, AFCRL-AFSIG-263
PROJ: AF-8624
TASK: 862401

UNCLASSIFIED REPORT

ABSTRACT: Research on vertically integrated boundary-layer winds applicable in Air Force paradrop operations required wind and temperature data taken on tall (higher than 250 ft) instrumented towers. The report represents findings from a search for such data. It provides an annotated listing of tall towers from which winds have been measured. The annotation consists of the following items when known: sensors used and their height; time periods over which measurements are averaged; data collection periods, format, and availability; other parameters concurrently measured on the tower; other boundary layer observations concurrently taken within a radius of about 20 mi; a listing of some studies using the data; and other pertinent information. (Author) (U)

DESCRIPTORS: (*TOWERS, *METEOROLOGICAL INSTRUMENTS), RADIO TOWERS, TELEVISION STATIONS, METEOROLOGICAL PHENOMENA, AIR DROP OPERATIONS, WIND, DETECTORS, STATISTICAL DATA (U)
IDENTIFIERS: METEOROLOGICAL TOWERS (U)

AD- 689 813 4/1

NEW MEXICO UNIV ALBUQUERQUE DEPT OF PHYSICS AND ASTRONOMY

STUDIES OF ATMOSPHERIC OZONE. (U)

DESCRIPTIVE NOTE: Final rept. 15 Mar 66-31 Dec 68,
MAR 69 171P Regener,Victor H. ;Aldaz, Luis ;
CONTRACT: AF 19(628)-5934
PROJ: AF-8631
TASK: 863102
MONITOR: AFCRL 69-0138

UNCLASSIFIED REPORT

ABSTRACT: The Final Report contains three papers entitled 'Turbulent Transport Near the Ground as Determined from Measurements of the Ozone Flux and the Ozone Gradient' by Victor H. Regener and Luis Aldaz; 'Flux Measurements of Atmospheric Ozone Over Land and Water' by Lius Aldaz; and 'Folded Optical Path of Great Length from Multiple Reflections Between Two Corner Cube Reflectors' by Victor H. Regener. The report also contains 205 computer-plotted graphs showing profiles of ozone, temperature and wind in the first 16 meters above the surface. These graphs contain a total of 382 profiles which were obtained on 37 days from December 22, 1966 to April 2, 1968. (Author) (U)

DESCRIPTORS: (*ATMOSPHERES, OZONE), TRANSPORT PROPERTIES, ATMOSPHERIC TEMPERATURE, WIND, MEASUREMENT, HEAT FLUX, DETECTORS, ATMOSPHERIC MOTION, TOWERS, DETECTORS, STRATOSPHERE, BOUNDARY LAYER, CHEMILUMINESCENCE, DATA PROCESSING, COMPUTERS, GRAPHICS (U)
IDENTIFIERS: GRAPHS(CHARTS) (U)

AD- 684 864 4/2 1/5

WEATHER BUREAU ATLANTIC CITY N J TEST AND EVALUATION LAB

ANALYSIS OF DESIGN CHARACTERISTICS OF METEOROLOGICAL TOWER FACILITY. (U)

DESCRIPTIVE NOTE: Final rept.,
JAN 68 100P Hochreiter, Frederick C. ;
PROJ: FAA-450-402-06E

UNCLASSIFIED REPORT

ABSTRACT: An analysis of design characteristics for an aviation oriented meteorological tower facility is discussed. The feasibility of converting an existing 150 ft. Air Height Surveillance Radar Tower is investigated. The study also incorporates an analysis of the instrumentation required to adequately describe the desired parameters, as well as sensor characteristics, spacing, orientation, and configuration, and the cost of such instrumentation. The feasibility of using the laser and aerosol measuring devices in the tower facility is discussed. Conclusions support the establishment of the Meteorological Tower test bed with a capability for measuring all parameters of interest to aviation terminal operations. The mass of the Tower gives it the stability necessary to affix components of transmissometer systems that will aid in slant visibility studies. (Author) (U)

DESCRIPTORS: (*METEOROLOGY, TOWERS), (*TOWERS, DESIGN), DETECTORS, INSTRUMENTATION, VISIBILITY, DEW POINT, STABILITY, RADAR, LASERS, AEROSOLS, WIND, ATMOSPHERIC TEMPERATURE, CLOUD COVER, ATMOSPHERIC MOTION, DATA PROCESSING, ANEMOMETERS, FEASIBILITY STUDIES, COSTS (U)
IDENTIFIERS: TRANSMISSOMETERS (U)

AD- 680 172 4/2

ATMOSPHERIC SCIENCES RESEARCH OFFICE WHITE SANDS MISSILE RANGE N MEX

A STUDY OF WIND AND TEMPERATURE VARIABILITY AT WHITE SANDS MISSILE RANGE, NEW MEXICO, (U)

SEP 68 40P Rider, Laurence J. ;
Armendariz, Manuel ; Hansen, Frank V. ;
PROJ: DA-1-T-061102-B-53-A
TASK: 1-T-061102-B-53-A-17
MONITOR: ECOM 5219

UNCLASSIFIED REPORT

ABSTRACT: Four cases of variation of wind and temperature over periods of approximately 12 hours in the first 152 meters of the planetary boundary layer are examined in some detail. An effort is made to explain some observed marked changes in wind and temperature which may not be apparent on the usual synoptic chart because of their mesoscale or microscale characteristic. (Author) (U)

DESCRIPTORS: (*WIND, DIURNAL VARIATIONS), (*ATMOSPHERIC TEMPERATURE, NEW MEXICO), VELOCITY, METEOROLOGICAL CHARTS, TOWERS, BOUNDARY LAYER, DISTRIBUTION, CLIMATE, BAROMETRIC PRESSURE, PERIODIC VARIATIONS, GUIDED MISSILE RANGES, WEATHER FORECASTING (U)
IDENTIFIERS: GRAPHS(CHARTS) (U)

AD- 526 618L 17/9

ARMAMENT DEVELOPMENT AND TEST CENTER EGLIN AFB FLA

Tower Test of Metal Sensor. (U)

DESCRIPTIVE NOTE: Final rept. 15 Dec 72-15 Jan 73,
JUN 73 35P Mannex,Henry R. ;
REPT. NO. ADTC-TR-73-38
PROJ: ADTC-679AA002

UNCLASSIFIED REPORT

Distribution limited to U.S. Gov't. agencies only; Test and Evaluation; Jun 73. Other requests for this document must be referred to Commanding Officer, Armament Development and Test Center, Attn: DLWG. Eglin AFB, Fla. 32542.

DESCRIPTORS: (*RADAR EQUIPMENT, TEST METHODS), RADAR RECEIVERS, DETECTORS, RADAR TARGETS, METALS, RANGE(DISTANCE), RADAR CROSS SECTIONS, CALIBRATION, RADAR ANTENNAS, RADAR TRANSMITTERS, TEST FACILITIES, TOWERS (U) *DOPPLER RADAR, *MOVING TARGET INDICATORS, SURFACE TARGETS, MOTION, POLARIZATION, DOPPLER EFFECT, RIFLES, TANKS(COMBAT VEHICLES), GROUND SPEED, ULTRAHIGH FREQUENCY (U)
IDENTIFIERS: M-16 RIFLES (U)

AD- 522 502L 20/5 17/8 (U)

ARMAMENT DEVELOPMENT AND TEST CENTER EGLIN AFB FLA

Laser Reflectivity Measurements. (U)

DESCRIPTIVE NOTE: Final rept. 8 Oct 71-22 Feb 72,
SEP 72 180P Curley,Dennis J. ;
REPT. NO. ADTC-TR-72-74
PROJ: ADTC-3169Y06A

CONFIDENTIAL REPORT
DECL- OADR

Distribution limited to U.S. Gov't. agencies only; Test and Evaluation; Sep 72. Other requests for this document must be referred to Commander, Armament Div., Attn: TESR. Eglin AFB, FL 32542.

DESCRIPTORS: (*LASERS, REFLECTIVITY), (*ELECTROMAGNETIC WAVE REFLECTIONS, SURFACE TARGETS), MEASUREMENT, ILLUMINATION, TRACKING CAMERAS, PHOTOTHEODOLITES, TOWERS, HELICOPTERS, OPTICAL TRACKING, DETECTION, RADIOMETERS, PORTABLE EQUIPMENT, CALIBRATION, INTENSITY, LIGHT TRANSMISSION, ENERGY, ATTENUATION, GRAPHICS, STATISTICAL DATA (U)

AD- 511 099 17/7 17/9

CORNELL AERONAUTICAL LAB INC BUFFALO N Y

ADLAT V (Advanced Low Altitude Techniques). (U)

DESCRIPTIVE NOTE: Final rept. 1 May 68-1 Jun 70,
AUG 70 259P Leney,Thomas F. ;
REPT. NO. CAL-IH-2635-E-4
CONTRACT: F33615-68-C-1641
PROJ: AF-5199
TASK: 519908
MONITOR: AFAL TR-70-150

CONFIDENTIAL REPORT
DECL- OADR

SUPPLEMENTARY NOTE: See also AD-500 113, AD-510 487 and AD-510 318.

DESCRIPTORS: (*TERRAIN AVOIDANCE, *RADAR NAVIGATION), VIDEO MAP MATCHING, VIDEO SIGNALS, HEIGHT FINDING, RADAR ANTENNAS, ANTENNA FEEDS, ANGLE OF ARRIVAL, DATA PROCESSING, AUTOMATIC, ACCURACY, RAINFALL, TOWERS, RADAR SIGNALS, LOW ALTITUDE, SIMULATION (U)

UNCLASSIFIED

DTIC REPORT BIBLIOGRAPHY SEARCH CONTROL NO. LTK53D

AD- 393 040 17/9

ARMAMENT DEVELOPMENT AND TEST CENTER EGLIN AFB FLA

EVALUATION OF THE AN/TPS-54 RADAR SET. (U)

DESCRIPTIVE NOTE: Final rept. 1 Apr-4 Jun 68,
AUG 68 54P Doubleday,Robert D. ;
REPT. NO. ADTC-TR-68-6
PROJ: ADTC-677AY3

CONFIDENTIAL REPORT
DECL- OADR
Distribution: No Foreign without approval of Commanding Officer, Armament Development and Test Center, Attn: ADTTY. Eglin AFB, Fla. 32542.

ABSTRACT: A field evaluation of the AN/TPS-54 radar set, which was designed to satisfy a need for a lightweight, highly mobile, ground-based surveillance radar, was conducted. No major deficiencies were found in the performance of the AN/TPS-54. Some minor inadequacies were found; however, they had little impact on the overall capabilities of the test item. It is recommended that the AN/TPS-54 radar set be considered for addition to the Air Force inventory. (Author) (U)

DESCRIPTORS: (*SEARCH RADAR, PERFORMANCE(ENGINEERING)), (*RADAR EQUIPMENT, SEARCH RADAR), AIR FORCE EQUIPMENT, MOBILE, GROUND SUPPORT EQUIPMENT, MOVING TARGET INDICATORS, DETECTION, COVERT OPERATIONS, AIR TRAFFIC CONTROL SYSTEMS, RELIABILITY(ELECTRONICS), MAINTAINABILITY, HUMAN FACTORS ENGINEERING, TOWERS, RADAR ANTENNAS, COMBAT SURVEILLANCE, ACCEPTABILITY (U)

DTIC REPORT BIBLIOGRAPHY   SEARCH CONTROL NO. LTK53D

AD- 389 655   17   1/3   (U)   17/4
17/9

CORNELL AERONAUTICAL LAB INC BUFFALO N Y

ADLAT IV. ADVANCED LOW ALTITUDE TECHNIQUES. VOLUME
II: TECHNICAL DISCUSSIONS.   (U)

DESCRIPTIVE NOTE: Final rept. Jun 66-Feb 68,
MAY 68   318P   Leney,Thomas F. ;Coombs,C.
C. ;
REPT. NO. CAL-IH-2096-E-7-Vol-2
CONTRACT: AF 33(615)-2795
PROJ: AF-5199
TASK: 519904
MONITOR: AFAL   TR-68-79-Vol-2

CONFIDENTIAL REPORT
DECL-   OADR
Distribution: No Foreign without approval of Air
Force Avionics Lab., Attn: AVNT. Wright-
Patterson AFB, Ohio 45433.
SUPPLEMENTARY NOTE: See also Volume 1, AD-389 656.

DESCRIPTORS: (*FLIGHT PATHS, *LOW ALTITUDE), SIMULATI(U)

APPENDIX B. COLLISION AND TERRAIN AVOIDANCE

AD-C028 856L 17/9 16/4

SPECTRA RESEARCH SYSTEMS NEWPORT BEACH CA

Adaptive Sensor Techniques for Target Coherence Enhancements. (U)

DESCRIPTIVE NOTE: Final technical rept. Mar-Dec 81,
APR 82 114P Kilday,B. L. ;Nicholas,L. W. ;Brewer,R. D. ;
REPT. NO. SRS-2680-82N
CONTRACT: F30602-81-C-0120
PROJ: LDFP
TASK: 01
MONITOR: RADC TR-82-97

SECRET REPORT
DECL- 31 Dec 93
Distribution: Further dissemination only as directed by RADC (OCTM), Griffiss AFB, NY 13441 or higher DoD authority.

DESCRIPTORS: *Doppler radar, *Terrain avoidance, *Guided missiles, *Cruise missiles, Atmospheric motion, Guided missile targets, Adaptive systems, Flight, Processing equipment, Time, Radar signals, Rejection, Requirements, Detectors, Signal processing, Performance(Engineering), Algorithms, Coherence, Approach (U)
IDENTIFIERS: Motion compensation, PE61101F, WURADCLDFP01C1 (U)

AD-C025 186 1/3 14/1

INSTITUTE FOR DEFENSE ANALYSES ARLINGTON VA SYSTEMS EVALUATION DIV

Cost Effectiveness of Alternative Configurations of Future Attack Helicopter Forces. (U)

DESCRIPTIVE NOTE: Final rept.,
JAN 81 153P Graves,James W. ;Durbin, Edgar ;Olver,Kelsey M. ;Zimmermann,Mark C. ;
REPT. NO. IDA-S-531
CONTRACT: MDA903-79-C-0320
MONITOR: IDA/HQ,SBI 80-22595,AD-E500 324

SECRET REPORT
DECL- OADR

ABSTRACT: The study evaluates the cost and effectiveness of several alternatives for the Advanced Attack Helicopter. The current AH-1S is considered together with several proposed modifications to its avionics and missiles. In addition to the AH-64, the Armed BLACK HAWK and a COBRA/HELLFIRE are also considered for the AAH role. Effectiveness estimates are made using the TETAM model for a variety of threat levels, terrain and visibility conditions, including likely battlefield obscurants. (U)
DESCRIPTORS: *Army aircraft, *Attack helicopters, *Cost effectiveness, Terrain avoidance, Configurations, Utility aircraft, Obscuration, Dust, Battlefields, Guided missiles, Threats (U)
IDENTIFIERS: TOW missiles, AH-1S aircraft, AH-64 aircraft, AH-1 aircraft, UH-60 aircraft, HELLFIRE missiles, LPN-IDA-PA/E-132 (U)

AD-A015 028 17/9 17/8 16/1 14/2

GEORGIA INST OF TECH ATLANTA ENGINEERING EXPERIMENT STATION

Instrumentation Techniques for Tracking Low-Flying Vehicles. (U)

DESCRIPTIVE NOTE: Final rept. 1 Sep 74-10 Jul 75,
JUL 75 135P Robinette,S. L. ;Rhodes,J. E. , Jr.;Wetherington,R. D. ;Reedy,E. K. ; Hayes,r. D. ;
REPT. NO. GIT-A-1678-F
CONTRACT: DAAD07-75-C-0025
PROJ: GIT-A-1678

UNCLASSIFIED REPORT

ABSTRACT: An anlysis and evaluation has been made of available range instrumentation which would permit White Sands Missile Range to measure performance of low-flying missiles and aircraft, with the following accuracy objectives: 10 feet in position, any axis; 5 feet per second, in velocity; and 5 feet per second in acceleration. A configuration was analyzed which used range measurements from ground sites to determine the position of an overflying aircraft, and tracking (measurements of range and pointing angles from the aircraft to the test vehicle) to determine the position of the low-flying vehicle. An inertial measurement unit, an altimeter, and a digital processor in the aircraft would establish attitude of the airborne reference system. No available airborne tracking equipment was found which would meet the White Sands Missile Range requirements. Both millimeter and laser airborne radars were evaluated as candidates for device development programs, to perform the function of airborne tracking. The possibility was examined of using an available Ku band airborne radar to determine altitude with 10 foot accuracy, the assumption being that higher horizontal position errors (approx 50 feet) could be tolerated. A ground based laser radar network, and a multilateration technique were analyzed. The latter would require range measurements from ground sites to the low-flying target, from the ground sites to an overflying aircraft, and from the aircraft to the low-flying target. (Author) (U)
DESCRIPTORS: *Guided missile tracking systems, (U)

AD-A015 028

AD- 784 376 16/4

JOHNS HOPKINS UNIV SILVER SPRING MD APPLIED PHYSICS LAB

Probability of Crashing for a Terrain-Following Missile. (U)

DESCRIPTIVE NOTE: Technical memo.,
APR 74 26P Cunningham,Edward P. ;
REPT. NO. APL-TG-1239
CONTRACT: N00017-72-C-4401

UNCLASSIFIED REPORT

SUPPLEMENTARY NOTE:
ABSTRACT: The report deals with the derivation of a new expression for PC, the probability of crashing, for a terrain-following missile. It is compared with the older, commonly used expression for PC. In general, it gives more pessimistic results; i.e., the missile must fly higher in order to achieve a probability of not crashing equal to that obtained by the older method. (Author) (U)
DESCRIPTORS: *Guided missiles, *Terrain following, *Flight control systems, Reliability, Terrain avoidance, Crashes, Probability, Altitude, Transfer functions (U)

AD- 784 376

AD- 531 105L 16/4.2 21/5 17/7 17/9
17/1 20/4 20/5 9/1

JOHNS HOPKINS UNIV SILVER SPRING MD APPLIED PHYSICS LAB

Research and Development Programs. (U)

DESCRIPTIVE NOTE: Quarterly progress rept. 1 Jan-31 Mar 74.
MAR 74 63P
REPT. NO. APL-C-RQR/74-1
CONTRACT: N00017-72-C-4401

CONFIDENTIAL REPORT
DECL- OADR
Distribution limited to U.S. Gov't. agencies only; Test and Evaluation; 1 May 74. Other requests for this document must be referred to Johns Hopkins Univ., Applied Physics Lab., Attn: Naval Plant Representative. Silver Spring, Md. 20910.

DESCRIPTORS: (*Weapons, *Naval research), (*Rocket ramjets, *Surface to surface missiles), (*Ramjet engines, *Guided missiles), Remotely piloted vehicles, Semiconductors, Radomes, Integrated systems, Atomic clocks, Reflectometers, Electronic countermeasures, Guidance, Air breathing engines, Jet engine inlets, Radar, Amorphous materials, Beam steering, Cooling, Terrain avoidance, External burning, Drag reduction, Projectiles, Solid propellants, Cavities, Laminar flow, Light scattering, Lasers, Radar antennas, Electrostatics (U)

AD- 531 105L

UNCLASSIFIED

DTIC REPORT BIBLIOGRAPHY SEARCH CONTROL NO. LTK50C

AD- 529 288L 17/7 16/4 (U) 19/5
16/4.1 15/3 17/9

RAYTHEON CO BEDFORD MASS MISSILE SYSTEMS DIV

Multi-Purpose Missile Guidance Design Study. Volume 4, System Design, Performance and Development. (U)

DESCRIPTIVE NOTE: Final rept. 8 Nov 72-Jun 73,
JUL 73 396P Slawsby,Nathan ;Surenian, Rouben ;Scott,Robert ;Casey,Lawrence ;Curley, John ;
REPT. NO. BR-7609-4
CONTRACT: F33615-72-C-2199
PROJ: AF-611A
MONITOR: ASD/XR 73-14-Vol-4

SECRET REPORT
DECL- OADR
Distribution limited to U.S. Gov't. agencies only; Test and Evaluation; Jul 73. Other requests for this document must be referred to Commander, Aeronautical Systems Div., Attn: XRT. Wright-Patterson AFB, Ohio 45433.
SUPPLEMENTARY NOTE: Prepared in cooperation with Martin-Marietta Aerospace Div. See also volume 5, AD-529 289L. DDC Form 55 not necessary for document request.
ABSTRACT: This volume contains a detailed description of the MPM baseline guidance system, including operational concept, guidance logic, system and subsystem block diagrams. Guidance system performance is estimated for each MPM mission for both benign and nonbenign conditions, and the guidance system packaging approach is described. The state-of-technology vis-a-vis the baseline guidance system design requirements is assessed, and an advanced development program is outlined. The impact on the baseline guidance system design of removing secondary missions is discussed, and avionic support requirements and aircraft compatibility are addressed. Guidance system reliability, maintainability, 10-year life cycle cost and nuclear survivability/vulnerability predictions are made. (Author) (U)
DESCRIPTORS: (*Guidance, Multimode), (*Guided missiles, Multiple operation), Reaction time, Base lines, Compatibility, Costs, Jet bombers, Fighter bombers, Guided missile antennas, Avionics, Dual mode (U)

AD- 529 288L

DTIC REPORT BIBLIOGRAPHY   SEARCH CONTROL NO. LTK50C

AD- 529 286L   17/7   16/4   (U)   19/5
16/4.1   17/9   15/3

RAYTHEON CO BEDFORD MASS MISSILE SYSTEMS DIV

Multi-Purpose Missile Guidance Design Study. Volume 2. System Performance Requirements.   (U)

DESCRIPTIVE NOTE: Final rept. 8 Nov 72-Jun 73,
JUL 73   54P   Spiliotis,Harry ;Cramer,Don ;Hamilton,Paul C. ;Slawsby,Nathan ;McLeod , Robert ;
REPT. NO. BR-7609-2
CONTRACT: F33615-72-C-2199
PROJ: AF-611A
MONITOR: ASD/XR   73-14-Vol-2

SECRET REPORT
DECL-   OADR
Distribution limited to U.S. Gov't. agencies only; Test and Evaluation; Jul 73. Other requests for this document must be referred to Commander, Aeronautical Systems Div., Attn: XRT. Wright-Patterson AFB, Ohio 45433.
SUPPLEMENTARY NOTE: Prepared in cooperation with Martin-Marietta Aerospace Div. See also Volume 3, AD-529 287L. DTIC Form 55 not necessary for document request.
ABSTRACT: This volume contains a derivation of missile and guidance system performance requirements for each MPM mission. Included are missile range, velocity, maneuverability, reaction time, radar cross section, miss distance (SEP/CEP), and terrain clearance requirements. (Author)   (U)
DESCRIPTORS: (*Guidance, Multimode), (*Guided missiles, Multiple operation), Range(Distance), Velocity, Dual mode, Maneuverability, Reaction time   (U)

APPENDIX C. GEORGIA TECH VISUAL MODEL

Computer graphics modeling techniques are providing a new tool for evaluating and improving the performance of military target acquisition and guidance systems.

An Infrared Background Clutter Model Using 3-D Computer Graphics

G. R. Loefer, D. E. Schmieder, W. M. Finlay, and M. R. Weathersby
Georgia Institute of Technology

The most difficult problem in locating and defining military targets by means of infrared acquisition systems is the presence of background clutter. This interference caused by natural and man-made objects confuses systems designed to find and track targets autonomously and places a severe limit on their performance. Many autonomous target acquisition and guidance systems are under development. They range from small and compact submunitions with limited processing power to large, powerful target screeners and map correlators. However, they all face the same problem—well before they reach their temporal noise sensitivity limits, these systems reach the performance limits imposed by the effects of background clutter.

There is need for an evaluation tool capable of both assessing system performance in clutter and increasing our understanding of clutter itself. The Georgia Tech Infrared Background Clutter Model[1] was developed for that purpose. It is intended to reduce dependency on flight testing for system evaluation, to permit system design optimization in the laboratory, and to provide insight into real-world clutter behavior.

The Georgia Tech model combines computer graphics and infrared physics to produce synthetic scenes with the statistical properties of real scenes. The scenes can be viewed from any geometry and include concave and convex surfaces as well as hidden objects. They may incorporate multiple illuminating sources for diffuse reflection or self-emission modeling. Targets, buildings, and other natural or man-made clutter objects can be inserted with any orientation anywhere in the scenes. The new model allows full simulation of varying depression angles, range closure, and fly-over.

Modeling of real scenes

Real scenes are composed of collections of different classes of objects. Although these collections can be either homogeneous or a mixture of classes, objects of the same class tend to be clustered spatially, and, together, these clusters form a large-scale scene structure, or macrostructure. One can model this structure by dividing a scene into regions of varying size and shape and recreating the properties of a single class of object for each region. Properties important in producing realistic scenes are the spatial structure (including class distribution, transition regions, texture, and 3-D effects), radiance statistics, and spectral distributions.

Radiance distributions of scenes containing an ensemble of background features resemble multimodal Gaussian distributions. This resemblance is caused by the fact that the background features have differing temperature means and deviations, but each feature has its own Gaussian distribution. The radiance of a feature is a function of both temperature and emissivity and is also Gaussian in nature. Figure 1 shows histograms illustrating these ensemble distributions. The top curve shows the histograms of the background features contained within the two small boxes (a,b); each has its own mean and devia-

0272-1716/83/0300-0055$01.00 © 1983 IEEE

tion. The bottom histogram is for the large box (c) and shows how a multimodal radiance distribution arises from an ensemble of homogeneous classes with different means. In fact, it can be shown that the statistics for an ensemble of different classes with homogeneous Gaussian intensity distributions produce a non-Gaussian distribution with mean μ_T and variance σ_T^2. The total statistics are related to the individual statistics by

$$\sigma_T^2 + \mu_T^2 = \sum_{i=1}^{m} \delta_i (\sigma_i^2 + \mu_i^2) \tag{1}$$

where

$$\mu_T = \sum_{i=1}^{m} \delta_i \mu_i$$

$$\delta_i = \frac{N_i}{N_T} \tag{2}$$

$$N_T = \sum_{i=1}^{m} N_i \tag{3}$$

N_i = number of pixels in class i, $N_i >> 1$
N_T = total number of pixels in scene
δ_i = fraction of scene for class i
σ_i = standard deviation for class i
μ_i = mean for class i
m = total number of classes in scene

The effect of each class on the ensemble statistics is directly related to the area (number of pixels) that class occupies. This leads to a more formal definition of a class

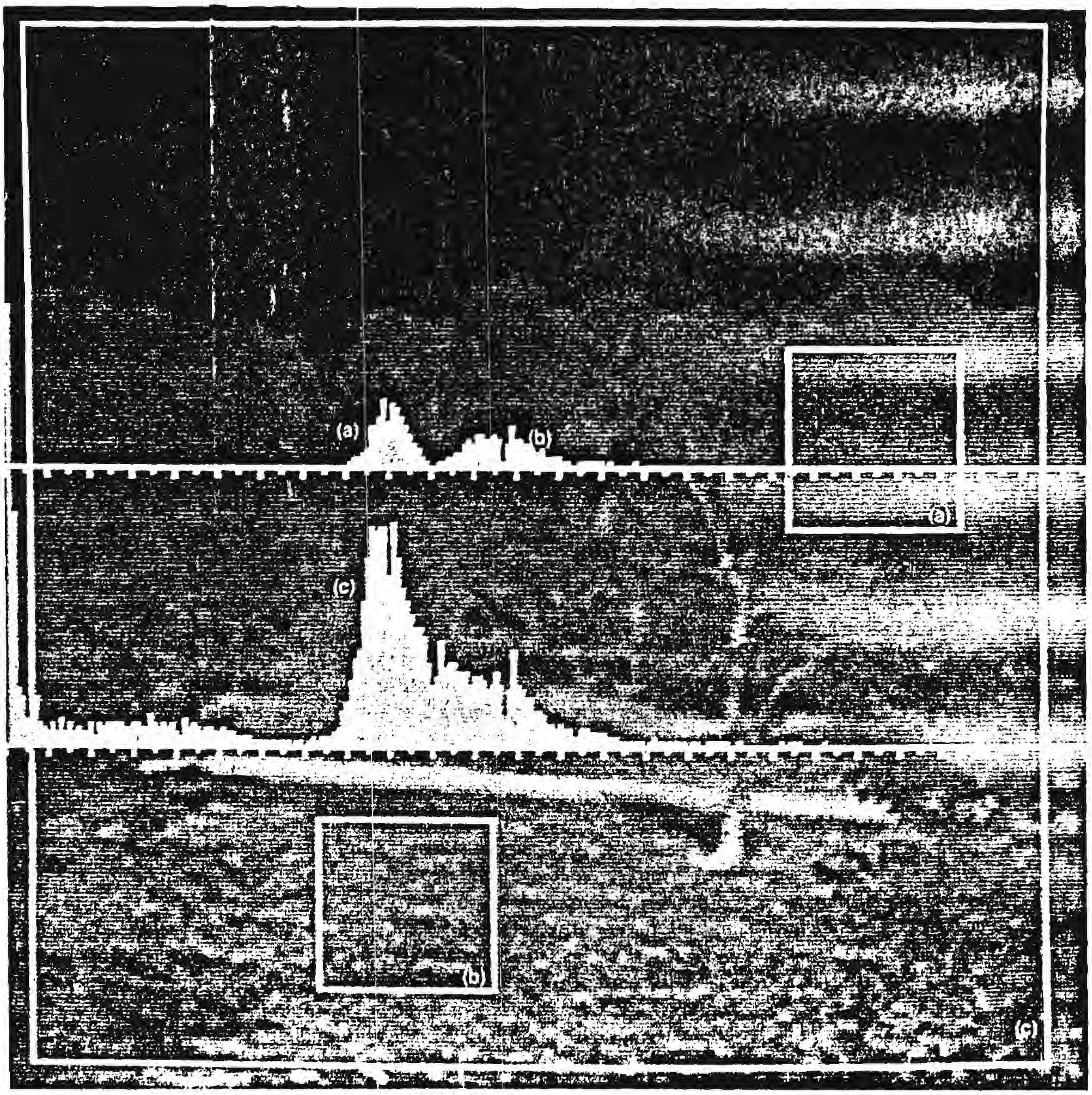

Figure 1. Radiance distribution. The top histogram is derived from features within the two boxes (a, b). The bottom histogram shows the radiance distribution of the whole scene within the large box (c).

as a set of spatially contiguous points with stationary radiance statistics. Observations to date have shown that these distributions are, in general, Gaussian.

The scene generation process calculates Gaussian radiance distributions for the various background objects by assigning different temperatures and emissivities to objects of different classes. Changes in ambient conditions can change both the radiance mean and deviation in varying degrees from class to class because differences in thermal mass and emissivity affect temperature distributions.

Transition regions between objects of different classes show special properties. In man-made features, the objects tend to be fairly homogeneous, with sharp transitions between classes (e.g., between a garage and a driveway). Natural features[2] generally tend to be less homogeneous with transitions characterized as spatially extended regions where two or more classes are mixed (a notable exception is the transition from water to land). The synthetic clutter model uses two methods to produce such features. First, the model varies object class boundary regions with a random spatial distribution to represent an irregular boundary in the direction parallel to the class transition region. Second, between homogeneous classes the model places regions of classes with properties of a mixture of the adjacent classes as determined by Equation 1. Examples of such mixed classes are readily seen in forests containing both deciduous and evergreen trees or in a weed-grown garden with patches of bare earth.[3] Such transition regions can be thought of as the spatial mesostructure of the scene.

Another spatial property is texture, or microstructure. Figure 2 shows a synthetic scene with different classes of texture. The scene synthesis model generates the various

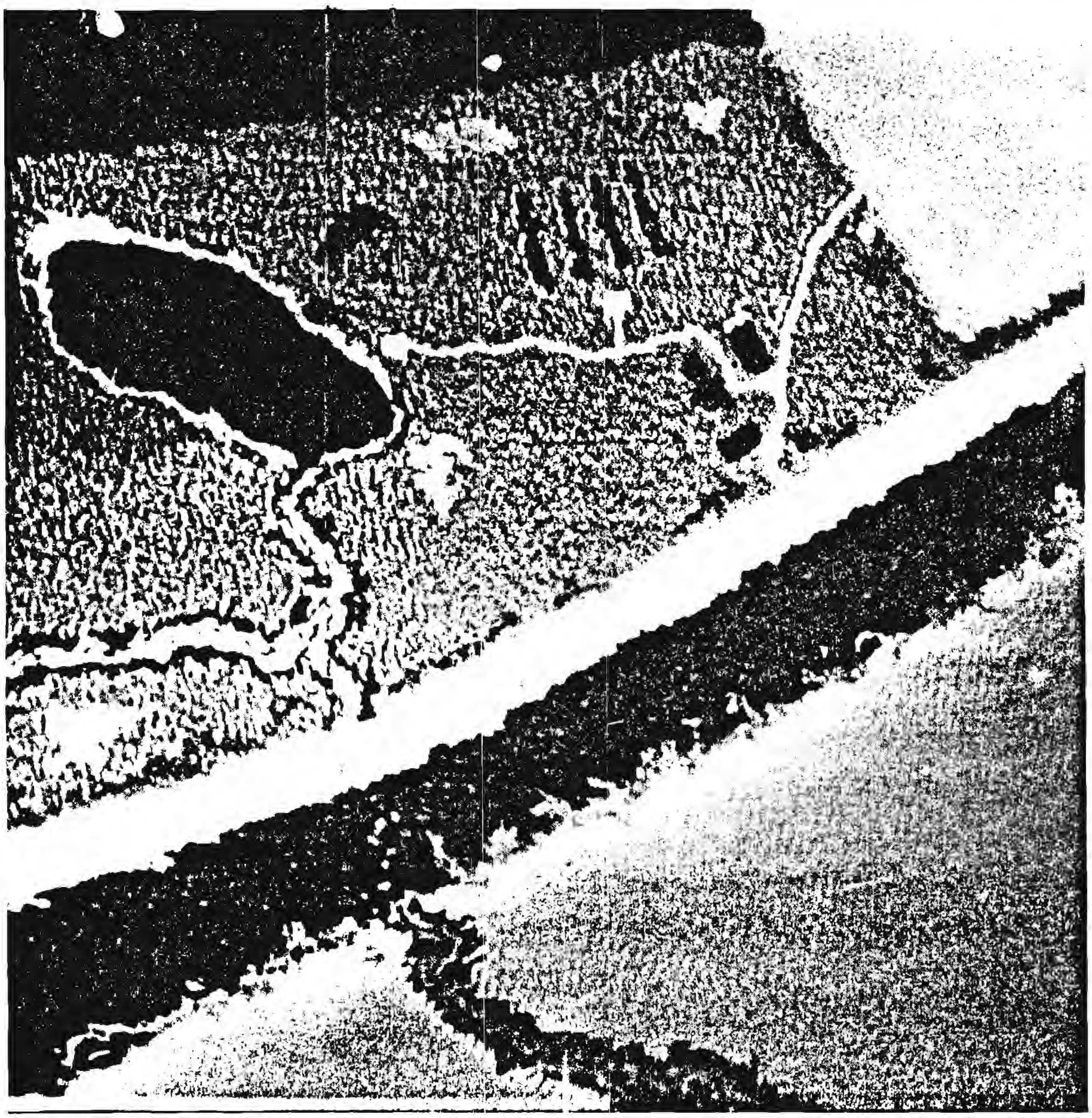

Figure 2. A synthetic scene with all classes assigned different properties demonstrates several classes of texture.

texture classes from a two-dimensional, autoregressive algorithm demonstrated by Haralick.[4] In the upper and lower quarter is a plowed open field with a furrowed texture. At the upper left and between the lower field and the road are regions of trees. The areas between the farm dwellings (right center) and the pond (left center) contain grass with two textures: long, coarse grass and short, mowed grass with a smoother texture. Each texture defines an autocorrelation length for each class. Designers of advanced sensors may use such textural features in target discrimination algorithms. These designers need textured scenes as a sensor evaluation tool.

Most real-world objects also exhibit widely varying appearance when viewed from different angles, due primarily to their three-dimensional anisotropy. Most 3-D effects can be modeled by using a topographic model. However, some natural objects (such as isolated trees) and most man-made objects (such as vehicles or bridges) cannot be modeled topographically since they are concave or multivalued at some or all grid points. A better approach to modeling these objects is to construct geometric solids from triangular facets. With these two approaches, changes in target signature and background clutter levels can be accurately modeled. The scene shown in Figure 3, for example, is a portion of the scene shown in Figure 2, viewed from a different angle.

Some sensors use multispectral acquisition/discrimination algorithms, for which proper spectral properties must be modeled. Up to this point, the scene generation process is independent of sensor characteristics; that is, class properties generated are random distributions of temperature. In order to calculate sensor response, the effective radiance in the proper spectral bands must be calculated from the wavelength response of the sensor(s), relative spectral emissivities for each class, and an atmospheric transmission curve. Multiplying these functions with blackbody functions and integrating the result produces a radiance map for each spectral band. This data is necessary in evaluating sensors that rely on information from more than one spectral region.

Structure, content, temperature, emissivity, texture, topography, and spectral radiance are important proper-

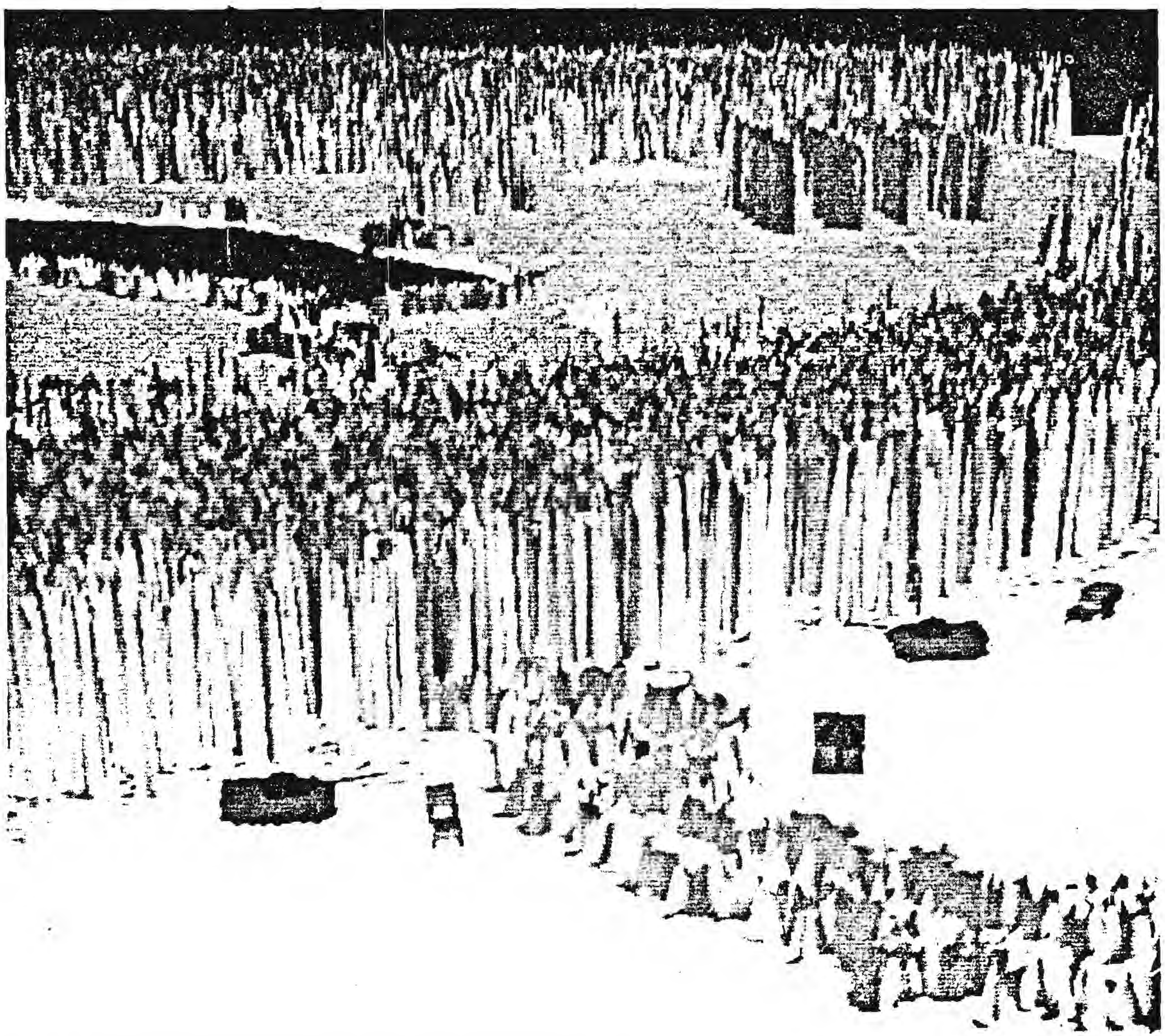

Figure 3. A synthetic 3-D scene complete with digitized targets.

ties of real scenes—they all must be accurately modeled to produce valid evaluation results.

Model Implementation

This section describes the key algorithms used during the modeling process. Figure 4 outlines the method of generating 3-D scenes containing targets. A class map is generated under supervisory control, using high-order irregular polygons to spatially distribute class values. Temperature and emissivity values, from which radiance is calculated, are modeled by generating random variables with Gaussian distributions characteristic of each class. Class statistics are controlled through a class table lookup. Topographic (height) data are also generated on a class-by-class basis. After selection of a viewing geometry, the 3-D projection is performed; a depth buffer performs hidden-object calculations. Finally, faceted models of targets and other objects can be added to complete the projected view.

Class-map generation. A class map is used to model two spatial properties of scenes. One of these properties, the IR (infrared) signature, is based on the premise that in the real world, similar objects are usually grouped together rather than scattered randomly. In other words, there exist patches of the same type of object. All individual objects of a class have nearly identical physical properties and therefore have similar IR signatures. Second, different classes mix along generally irregular spatial boundaries. Experience has shown that one key to producing realistic scenes is to recreate these irregular spatial boundaries between classes. A class map provides the necessary control over these two important spatial processes.

The class map defines regions of a single type of object and determines the extent and distribution of objects in a scene. In the present Georgia Tech model configuration, the class map is generated via a highly interactive program. Areas of classes are created under operator control of parameters that generate high-order, irregular polygons. The vertices of the polygons are generated by adding a controlled, random variability to regular 2-D polygons.

One of the most useful formulations for generating the polygons is the following equation, which has been dubbed the "superellipse"[5]:

$$\left(\frac{|x|}{a}\right)^{\alpha} + \left(\frac{|y|}{b}\right)^{\alpha} = 1 \qquad (4)$$

where

a, b are the semiaxes;
α can have any positive real value; and
x, y are vertex coordinates.

Equation 4 generates pairs of x, y coordinates. A random variability is introduced by using the x, y pair as the mean value of a bivariate Gaussian distribution in spatial coordinates. For the ith vertex

$$x_i' = \sigma_x \cdot A + x_i \qquad (5a)$$

$$y_i' = \sigma_y \cdot B + y_i \qquad (5b)$$

where

x_i, y_i = the coordinates of the ith vertex of the regular polygon determined by Equation 4
σ_x, σ_y = spatial standard deviations
A, B = normalized Gaussian random variable (zero mean, unit variance) from pseudorandom number generator
x_i', y_i' = randomized vertex coordinates

A family of superellipses with constant a and b and variable α is shown in Figure 5.

In the real world, similar objects are usually grouped together rather than scattered randomly.

After the polygon vertices are generated, the area covered by the polygon is assigned a class number by which all class properties are indexed. A polygon-filling program that addresses the map matrix in a line-by-line raster mode loads the class map. From the ordered set of vertex coordinates, the fill program calculates the number and extent of segments interior to the polygon. The polygon may be irregular, concave or convex, or even a collection of several disconnected regions (i.e., the sides of the polygon may intersect each other).

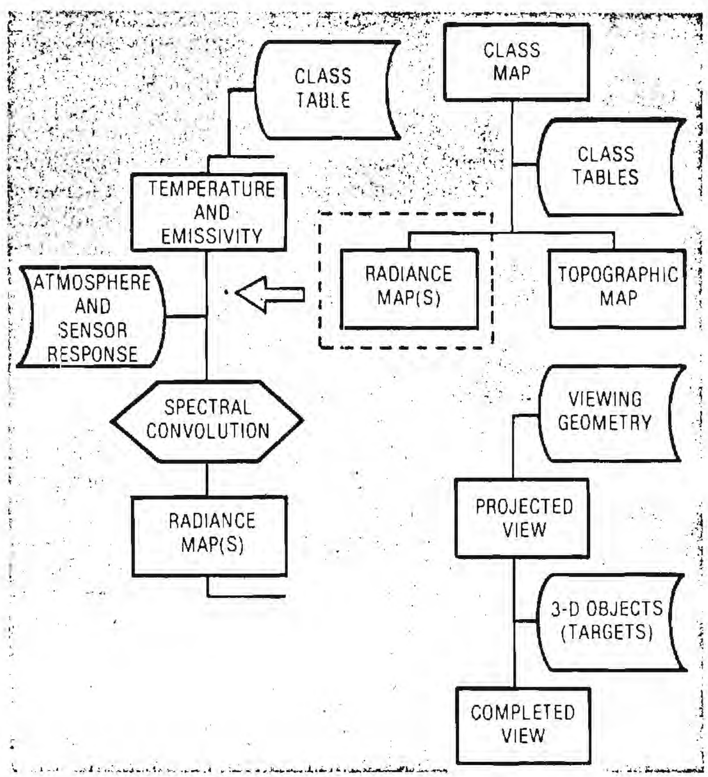

Figure 4. Flowchart of the complete 3-D scene generation process. The chart on the left is a detailed description of the process enclosed in the dotted box on the right.

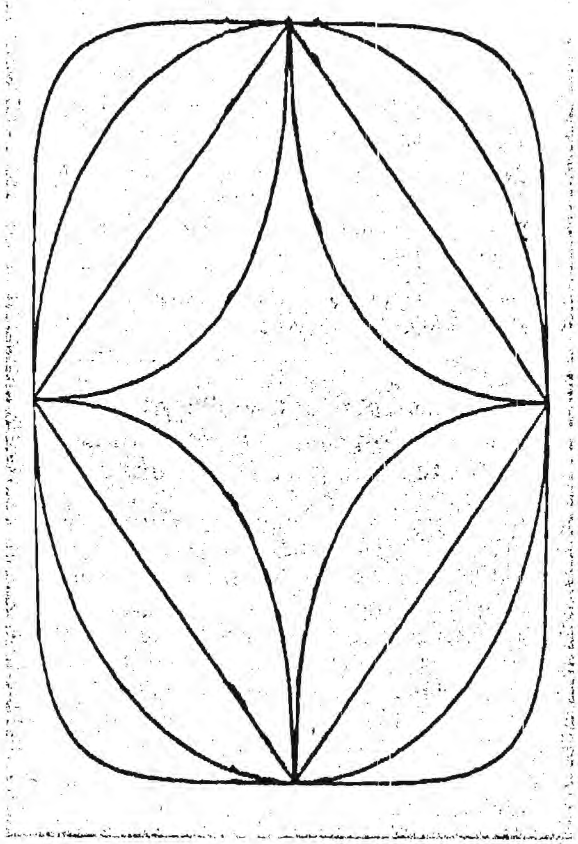

Figure 5. Superellipses. A wide variety of shapes can be generated from the superellipse equations. These curves have the same semiaxes but have different values of the exponential coefficient.

Use of the randomized polygons masks most but not all of the unnatural regularity of the basic superellipse. Further blending of classes and the addition of streams and rivers is accomplished by using an operator-controlled cursor to change values in the class map. This enhances boundary irregularities and allows insertion of areas for mixed classes of transition regions. Figure 6 is a typical class map.

The main purpose of the superellipse is to rapidly fill large, contiguous areas of the class map with a single number, while maintaining operator control over shape, size, location, and boundary irregularity. Some of these forms must be regular in order to reproduce man-made features. Fractal curves could provide some (but not all) of these features. The superellipse can produce a wide variety of forms with only a few parameters. Fractal curves and fractional Brownian motion are being investigated as enhancements for the generation of detailed topography and texture.

Production of the class map is labor intensive and is not limited by the speed of the algorithms but by the decision process of the operator. The generation of the class map represents a relatively small portion of the scene generation process, as a single class map can be used to produce many different scenes. (All the scenes illustrating this article were produced from a single class map.)

Radiance-map generation. Once the master scene has been defined by the class map, a wide variety of ambient conditions, scene content, and scene complexities can be generated with a class parameter lookup table. This table contains the parameters controlling temperature and emissivity statistics, which, in turn, control radiance mean and standard deviation for all classes. These parameters can be derived from a phenomenological model, empirically measured, or arbitrarily assigned. For each scene, the class map is scanned pixel by pixel, and each pixel is assigned a temperature and emissivity (in one or more bands), which is Gaussian-distributed according to the class table parameters. If there is a known correlation coefficient between two spectral bands, then the emissivity values in both can be generated by the expression[6]

$$\begin{aligned} \epsilon_1 &= \mu_1 + \sigma_1 A \\ \epsilon_2 &= \mu_2 + \sigma_2(\rho A + \sqrt{1-\rho^2}\,B) \end{aligned} \tag{6}$$

where

A, B = normalized Gaussian random variables
μ_1, μ_2 = emissivity mean value in spectral bands 1 and 2 respectively
σ_1, σ_2 = emissivity standard deviation in spectral bands 1 and 2 respectively
ρ = spectral correlation coefficient (band 1 to band 2)
ϵ_1, ϵ_2 = emissivity in spectral bands 1 and 2 respectively

The use of Gaussian distributions of temperatures and emissivities has proven effective in producing radiances with Gaussian distributions, as one would expect from published data, primarily because real-world temperature differences (ΔT's) are on the order of a few degrees Celsius. For these small ΔT's, the radiance integrated over the typical IR spectral bands is approximately linear and does not significantly distort the measureable IR signatures. The effect of larger ΔT's on radiance statistics and correlation (or lack thereof) remains a difficult issue.

The effect of large real-world temperature differences on radiance statistics and correlation remains a difficult issue.

The radiance map thus models the IR self-emissions of the scene as viewed at the nadir. Masking and aspect projections must be handled by the 3-D projection model, which can also handle simple reflections from several point sources.

Topography generation. The class tables also contain parameters that characterize variations in object heights, providing mean heights and standard deviations for each class of object in the same manner as they provide temperature and emissivity values. The height of any given grid cell, h, is calculated by

$$h = \mu_h + \sigma_h A \quad (7)$$

where

μ_h = object mean height

σ_h = object height standard deviation

A = normalized Gaussian random variable

h = cell height

These heights are used as inputs to the 3-D projection model.

Scene projection. The projection model simulates the three-dimensional nature of the real world. The appearance of a scene can change drastically over different viewing geometries. These changes include obscurations of one object by another, perspective projections, and range-dependent effects such as haze or fog.

The three-dimensional projection model treats the gridded topographic database as a sampled, continuous sheet. The grid coordinates are assumed as x and y and the topographic data (height) as z. The projection produces information on cell image coordinates, distance to the observer, and angles between surface normals, sources, and the observer. The cell intensity can be modeled as any function of these parameters. Thus, both self-emission and reflected radiation from multiple point sources can be modeled.

All the data associated with the class map, such as topography, radiance, temperature, and emissivity, is stored in a regularly gridded format. To perform a particular projection from the topographic database, a viewing geometry must be defined. The viewing geometry contains four parameters: (1) the position of the obser-

Figure 6. A typical class map. Each intensity represents a different class. Note the varied edges on different classes.

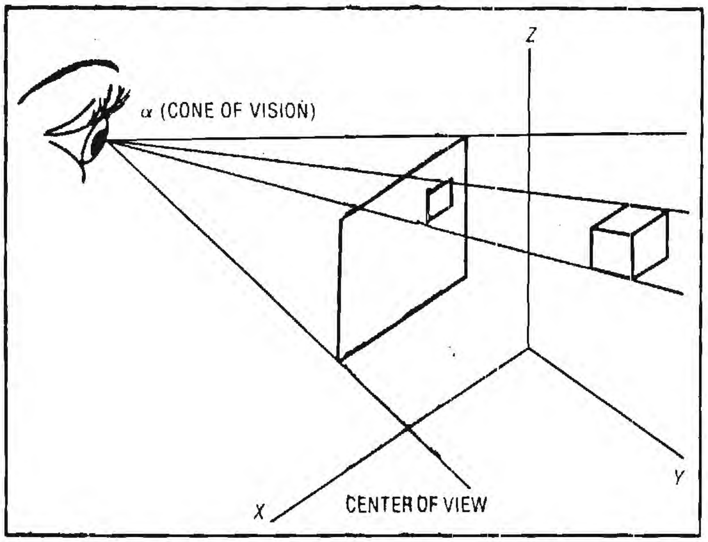

Figure 7. Perspective projection. A simple calculation using similar triangles maps a point in three-space to the two-dimensional viewing plane of the observer.

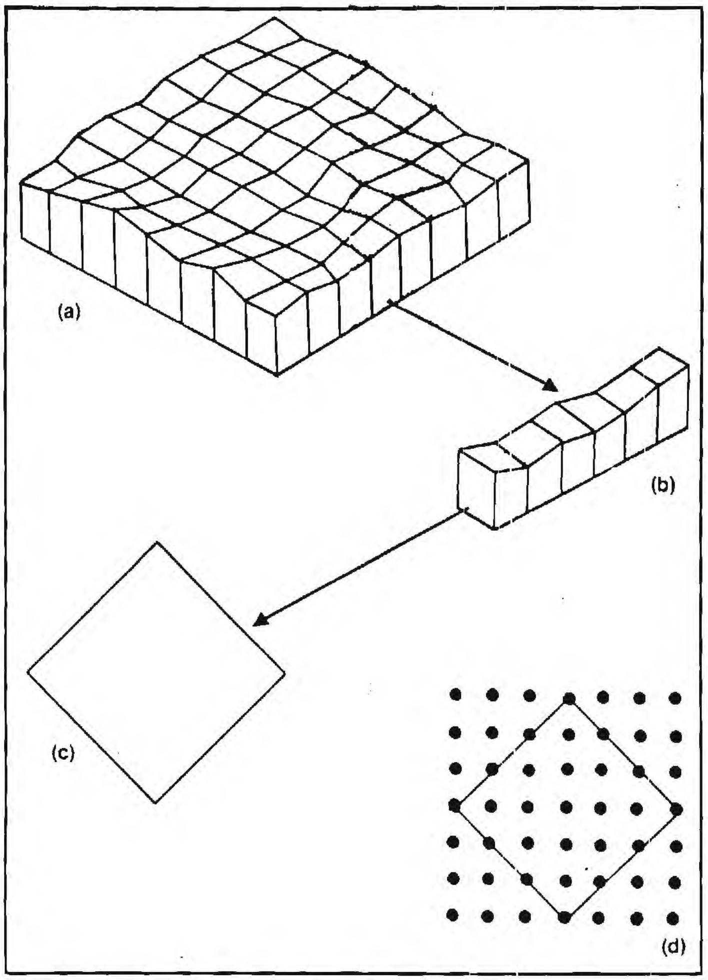

Figure 8. Projecting the topographic surface. The complete surface with overlaid grid (a) is projected a row at a time (b). Adjacent rows define the grid cells, which are processed one at a time (c). The projected cell is overlaid onto the screen image (d). Interior shading is computed by interpolation from the corners.

ver, (2) the "center of view"—a point in the database that will be at the center of the three-dimensional projection, (3) the field of view, and (4) source positions. The field of view specifies a cone of vision defining the final perspective (see Figure 7). Once these parameters are defined, any point in three-space can be mapped to a point in the projection (two-dimensional image) with a simple linear transformation. The field of view also defines the region of topography that could possibly be projected on the screen. This eliminates much of the database from consideration for close viewing geometries, thus reducing required computations.

For the 3-D projection, topographic data is processed three adjacent rows at a time. For each point in the topographic grid, a surface normal is estimated with a least-square computation based on the surrounding eight points. The surface normal for point (m,n) is estimated by computing the least-square approximation of a plane to the eight points about (m,n). The estimation of the surface normal is

$$\hat{S}_{(m,n)} = (\hat{x}, \hat{y}, \hat{z}) \tag{8}$$

$$Z = 1$$

$$X = \tfrac{1}{3} \left(\sum_{i=-1}^{+1} \left(Z_{(m-1,\, n+i)} - Z_{(m+1,\, n+i)} \right) \right)$$

$$Y = \tfrac{1}{3} \left(\sum_{i=-1}^{+1} \left(Z_{(m+i,\, n-1)} - Z_{(m+i,\, n+1)} \right) \right)$$

where this vector must then be normalized to have unit length.

After surface normals have been calculated, each cell must be projected and assigned intensity(ies). Associated with each point in the grid, there is a height, a radiance value, a class value, and an estimated surface normal to be used in the projection. The projection model uses two of the three rows of topography and surface normals at a time. A set of four-sided cells is defined by these two adjacent rows, as shown in Figure 8. Each corner of the cell is projected with a simple perspective transformation, thus defining a four-sided polygon in the two-dimensional image. In order to make a solid image, the interior of this polygon must be filled with a value corresponding to the type of radiance model being used. This value may be a function of the class, radiance, temperature, surface normal at the point, or any combination of these. Only the values at the polygon vertices can be computed directly, as these correspond to points in the grid. The interior points of the polygon correspond to points between the grid points and so must be estimated.

The model used to estimate the intensities in the interior of the polygons is an implementation of the Gouraud shading algorithm.[7] This model is exact for shading cells whose intensities are independent of surface-normal orientation. It also provides an excellent approximation to intensities that do depend on surface normals and is significantly faster computationally than other, more exact models.[8] Inaccuracies in the Gouraud shading algorithm occur for highly symmetrical objects.

Real-world topography rarely contains such objects and thus the more computationally intensive Phong algorithm is unnecessary. In fact, both algorithms have been used to produce a variety of scenes and the resulting images are indistinguishable.

To create a realistic scene, a projection model must take hidden surfaces into account. The Georgia Tech model accomplishes this by using an enhancement to the depth buffer approach as described by Newman and Sproull.[9] The depth buffer approach accounts for hidden surfaces by using a "painter's algorithm." As each topographic grid cell is projected, the distance from the observer is computed for each point in the projected image of the polygon. Each new point's distance is compared to the distance for the point stored in the depth buffer at the same image coordinate. If the new point is closer, it replaces—"paints over"—the stored value. Otherwise, the new point must be hidden and is not saved. Typically, the depth buffer contains only range and intensity. The unique feature of the Georgia Tech approach is that when a point is saved, three pieces of information about the point are stored in the depth buffer:

To create a realistic scene, a projection model must take hidden surfaces into account.

(1) an interpolated intensity value,
(2) a class number, and
(3) a distance from the observer to the point.

Although these three parameters are all that are currently stored, there is no conceptual limit to the type of data that can be stored in the depth buffer. This approach allows flexibility to incorporate other information should models of other phenomena require different data types.

The Georgia Tech depth buffer has several major advantages over other methods:

(1) Computations are simple. No elaborate hidden surface calculations are required.

(2) Data is processed in a raster method, no matter what viewing geometry is used. When processing is complete, the depth buffer contains the projected image, also in raster format.

(3) The depth buffer contains more information than the projected scene intensities. The storage of distance data allows new features such as targets, trees, and new scene segments to be added to the scene at any time. It also allows simplified modeling of atmospheric effects. By preserving class numbers, the depth buffer provides exact ground truth for every pixel of the projected image. Also, storing class numbers allows use of alternate intensity models without the need for additional projection calculations. Using a depth buffer makes the scene projection process interruptible and fully reentrant.

Only the first two points are true of depth buffers as they are generally used. The third feature is unique to the Georgia Tech approach. Adding other information to the depth buffer gives the model a great deal more flexibility in displaying the generated scene under various simulated conditions.

3-D object generation and insertion. For many scenes, a topographic projection produces a satisfactory output. However, some objects, such as trees and vehicles, are not well represented by such a model, and a faceted model must be used (see Figure 9).

These models describe an object as a series of triangular facets in some arbitrary coordinate system, usually based at the center of the object. The models can be created either synthetically, as discussed in the next section, or by using a digitizer and multiple orthogonal views of real objects. In the latter method, a series of common points is found in the views, from which the program computes coordinates of triangles that make up the object in three-space. The amount of digitizing can usually be significantly reduced by exploiting the symmetry of a partially digitized object through the use of reflections and rotations to complete it.

As each triangular plate is generated, it is assigned a class value to designate what part of the object it represents. For example, in a model of a tank, a piece from the turret can be assigned a class value of 1, a piece from the gun a 2, from the wheels a 3, and so forth. Any facet may be assigned any class value. When the object is added to the scene, the class values are referenced to a radiance or intensity model, which is used for drawing. This technique allows for control of the overall target radiance or intensity, as well as variations of these parameters from one piece to another. Any target condition, such as running (hot engine compartment) or firing (hot barrel), with positive or negative contrast, can be simulated.

As the object is being added, the intensity is computed for each triangular plate from the class value and/or orientation of the plate. Unlike the original scene projection, no interpolation is possible because the triangular plates are in no particular order (i.e., they are not necessarily contiguous plates). This intensity is held constant for the whole plate. A smoother-looking object can be created by digitizing finer triangles, at the cost of more processing time and a larger data file.

Synthetic 3-D objects. Objects such as trees are much easier to synthesize than to digitize from real specimens. The synthetic object generation program creates realistic 3-D objects in the same faceted format as digitized objects (see Figure 10). The algorithm used by the class map generator to create irregular 2-D polygons can be extended to three dimensions to create faceted 3-D objects. The vertices are first created in a single plane, which is considered to be a meridian of an ellipsoid. Slight random variations around the meridian generate a set of vertices in three-space. Additional meridians are generated until the set of vertices is completed. The object is completed by converting the set of vertices into an ordered set of triangular facets suitable for input to the object insertion program. By variation of a few parameters, many types of trees, tree trunks, buildings, and regular geometric solids can be generated. With the insertion of all desired 3-D objects, the scene generation process is complete.

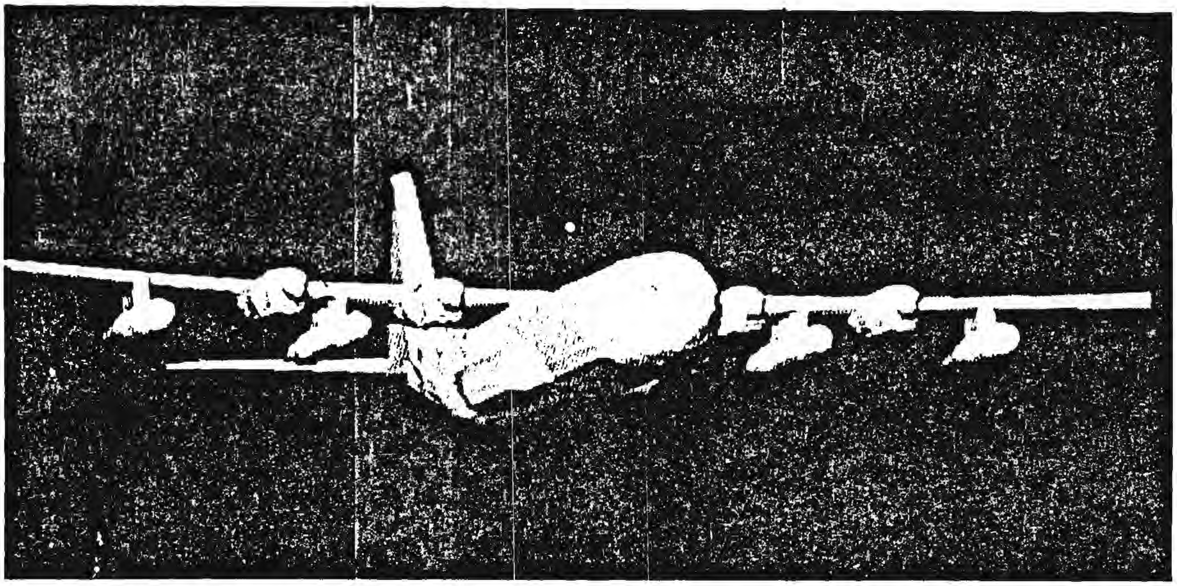

Figure 9. Faceted model. This digitized model of a cargo plane required over 4000 triangular facets.

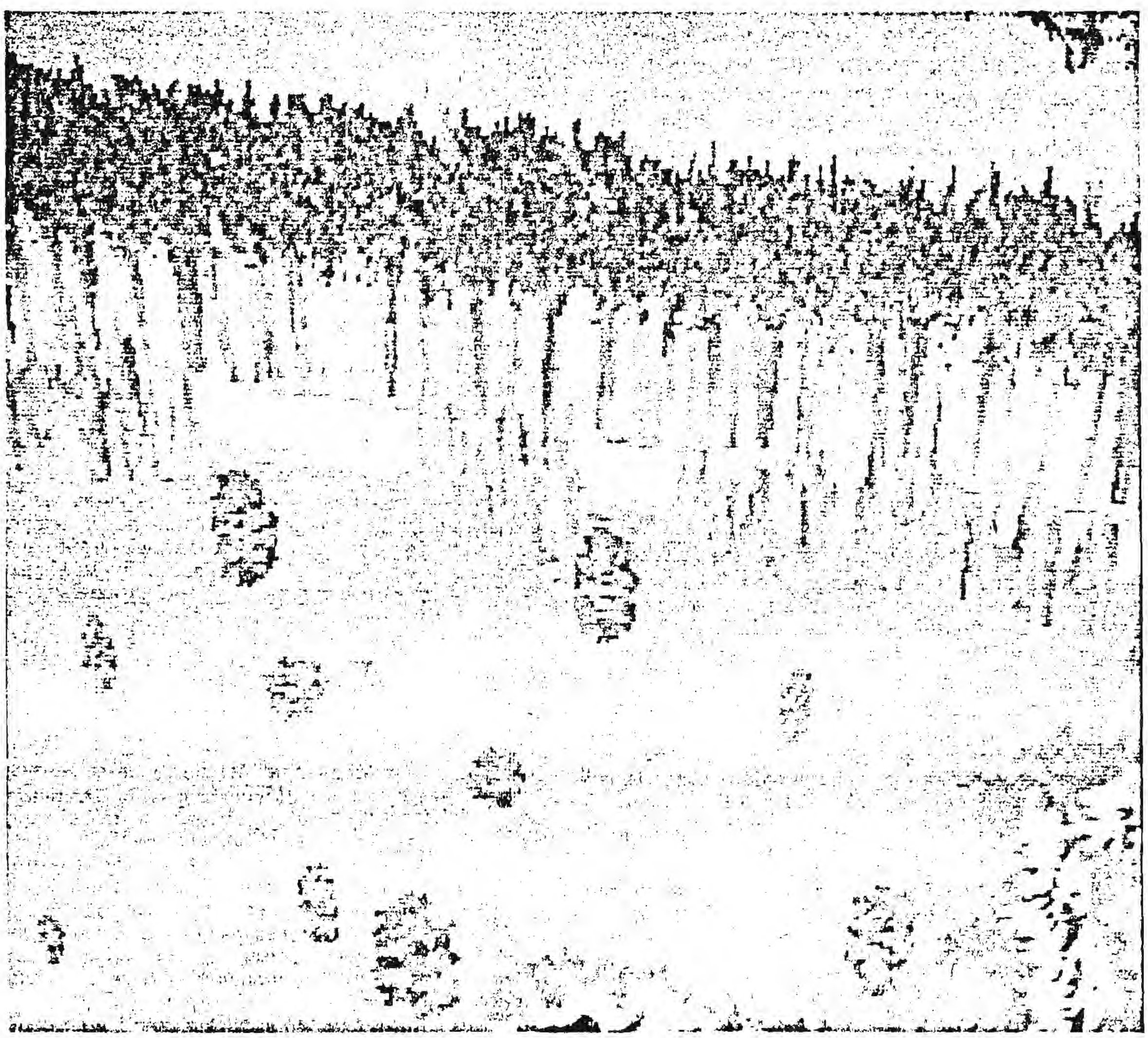

Figure 10. Synthetic trees. This scene contains both topographic trees (top) and faceted, synthetic trees (foreground).

Summary

The Georgia Tech model is a highly versatile model of infrared backgrounds and clutter. It uses class structures to produce synthetic scenes with the same amplitude, spatial, and spectral properties found in real scenes. A convenient and powerful tool for infrared system evaluation, the clutter model can be used to evaluate autonomous target acquisition, correlation guidance, and screener algorithms. It can help determine camouflage effectiveness and provide synthetic imagery for system simulation. Moreover, it performs these tasks with an efficient, fast-running computer code, without encountering the expense, uncertainty, and delay of flight test programs.

This background clutter model attempts to overcome two significant problems encountered with other modeling approaches: (1) a loss of realism due to oversimplified statistical assumptions and (2) a loss of convenience due to cumbersome algorithms that attempt to model all the detailed physical processes involved. The present model is designed to deterministically generate scene macrostructure, avoiding oversimplified statistical approaches. Moreover, the model relies on scaling laws and operator interaction to duplicate the results of physical processes accurately. Thus, the operator must choose the values for a few key statistical parameters from observed trends in real scene behavior. These parameters include such typical object class descriptors as temperature mean and standard deviation, topographic mean and standard deviation, and spectral emissivity. This approach uses the minimum amount of phenomenological modeling required to produce accurate outputs. In short, the goal of the Georgia Tech model development effort is to create realistic scene images and still maintain a practical, easy-to-use implementation. ■

Notes and references

1. Gene R. Loefer and David E. Schmieder, "Infrared Background Clutter Model," *Proc. IRIS Specialty Group on Targets, Background and Discrimination*, Aug. 1980, pp. 341-352.
2. Such features can be seen in almost any IR database, such as the Eglin AFB TABILS database, ADTC/DLMT. Georgia Tech clutter model development has also used the following data sources: US Army Micom AGA Thermovision 3-5 μm data from Aberdeen, Md., and Ft. Hood, Tex.; and US Army Night Vision Lab 8-12 μm data.
3. Mixed classes are commonly seen in Landsat earth resources satellite data.
4. Robert M. Haralick, "Statistical and Structural Approaches to Texture," *Proc. IEEE*, Vol. 67, No. 5, May 1979, pp. 798-804.
5. Martin Gardner, "The Superellipse: A Curve that Lies Between the Ellipse and the Rectangle," *Scientific American*, Sept. 1965, pp. 222-234.
6. D. E. Knuth, *The Art of Computer Programming*, Vol. 2, Addison-Wesley, Reading, Mass., 1969, p. 113.
7. Henri Gouraud, "Computer Display of Curved Surfaces," tech. report UTEC-CSc-71-113, Dept. of Computer Science, Univ. of Utah, June 1971; NTIS AD-762-018; abridged version in *IEEE Trans. Computers*, Vol. C-20, No. 6, June 1971, pp. 623-629.
8. Bui-Tuong Phong, "Illumination for Computer Generated Images," tech. report UTEC-CSc-73-129, Dept. of Computer Science, Univ. of Utah, July 1973; NTIS AD-A-008-786.
9. William M. Newman and Robert F. Sproull, *Principles of Interactive Computer Graphics*, 2nd ed., McGraw-Hill, New York, 1979.

Gene R. Loefer has been a research scientist with the Engineering Experiment Station of the Georgia Institute of Technology since 1975. His research interests include digital and hardware simulations of infrared systems, targets, and backgrounds; electro-optical systems analysis; and optical design.

Loefer received both the BS in physics and the MS in applied physics from the Georgia Institute of Technology. He is a member of OSA.

David E. Schmieder is acting chief of the Electro-Optics Division, Electromagnetics Laboratory, at the Georgia Institute of Technology Engineering Experiment Station. He was a staff engineer at Martin Marietta from 1972 to 1979. His technical interests include electro-optical systems analysis, sensor design, pattern recognition, and infrared countermeasures.

Schmieder received the BS in physics and mathematics from the University of Wisconsin at Platteville and the MS in physics from Kansas State University. He is a member of the IEEE, SPIE, and OSA.

William M. Finlay is a research scientist with the Engineering Experiment Station at the Georgia Institute of Technology. His research interests include three-dimensional computer graphics, sensor evaluation and modeling, and digital database analysis.

Finlay received the BS in mathematics and the BS in physics from MIT. He is a member of the MAA.

Marshall R. Weathersby is a research scientist with the Engineering Experiment Station, Electromagnetics Laboratory, at the Georgia Institute of Technology. Formerly he worked for Martin Marietta Aerospace. His research interests include design and applications of infrared and millimeter wave imaging systems, electro-optical countermeasures, image enhancement, target acquisition algorithms, and computer-generated imagery.

Weathersby received the BS in physics from Florida State University. He is a member of the IEEE, the APS, the AOC, and Phi Beta Kappa.

APPENDIX D. SYNTHETIC DATABASE SAMPLES

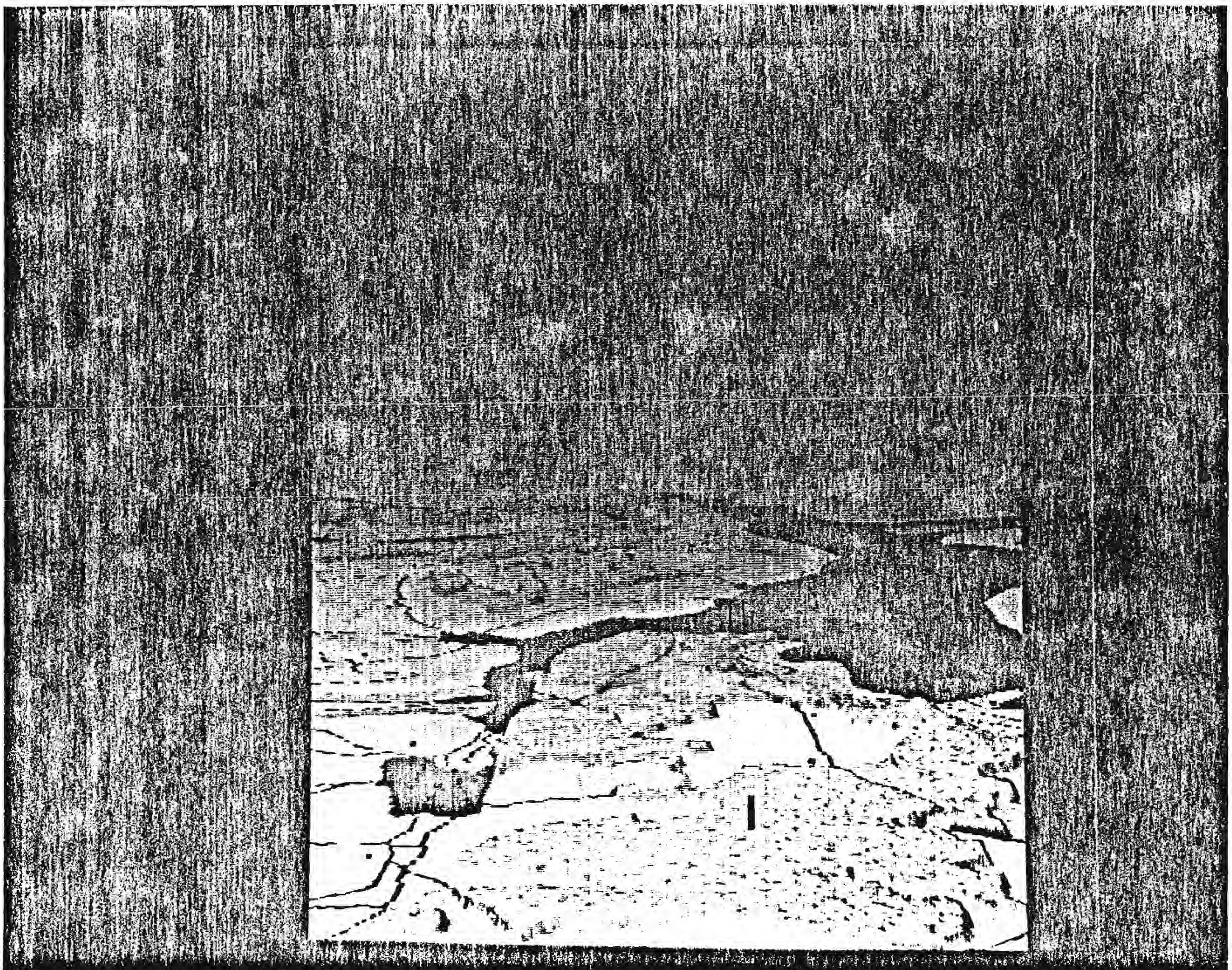

FIGURE D.1 SYNTHETIC IMAGERY - DISTANT

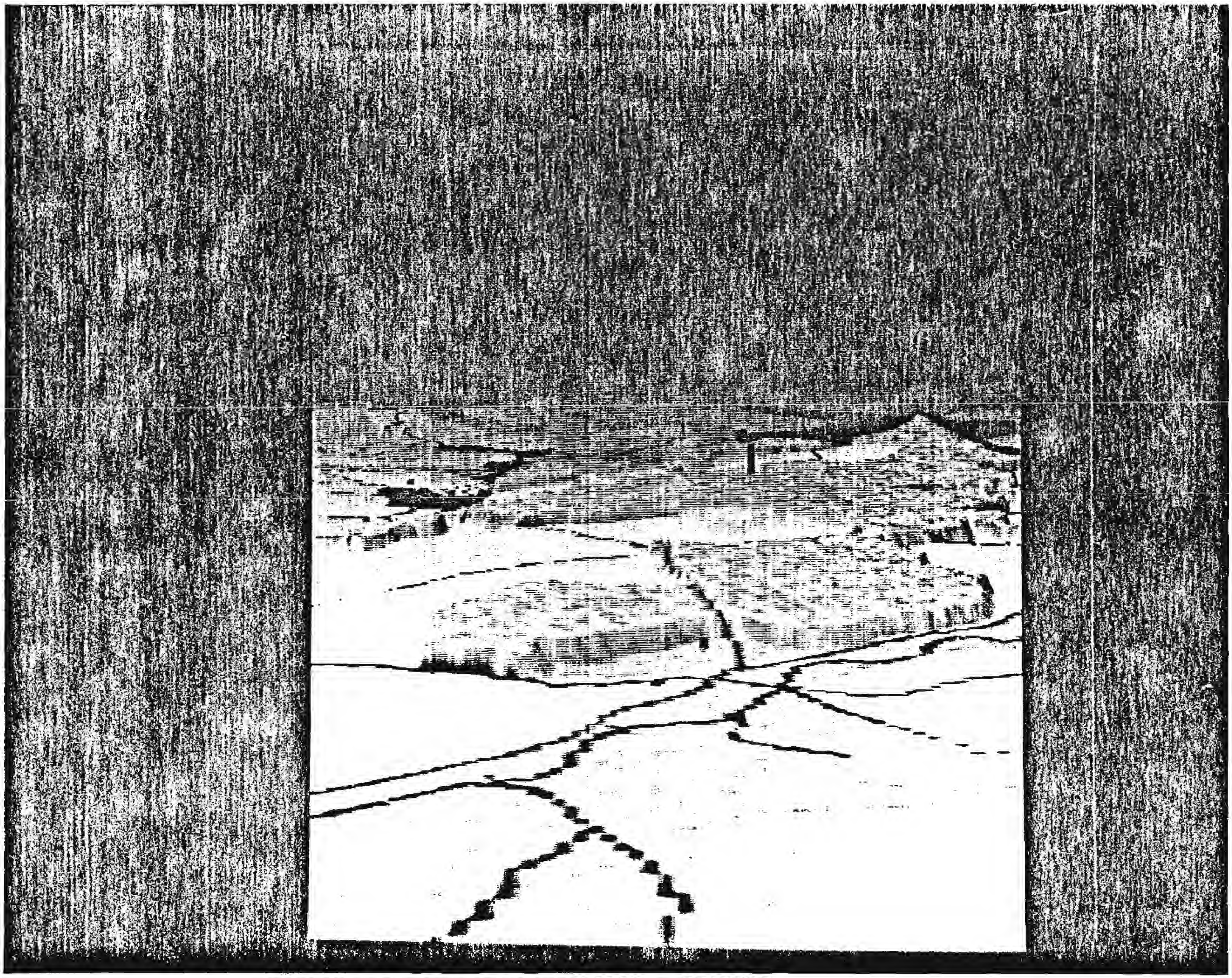

FIGURE D.2 SYNTHETIC IMAGERY - DISTANT

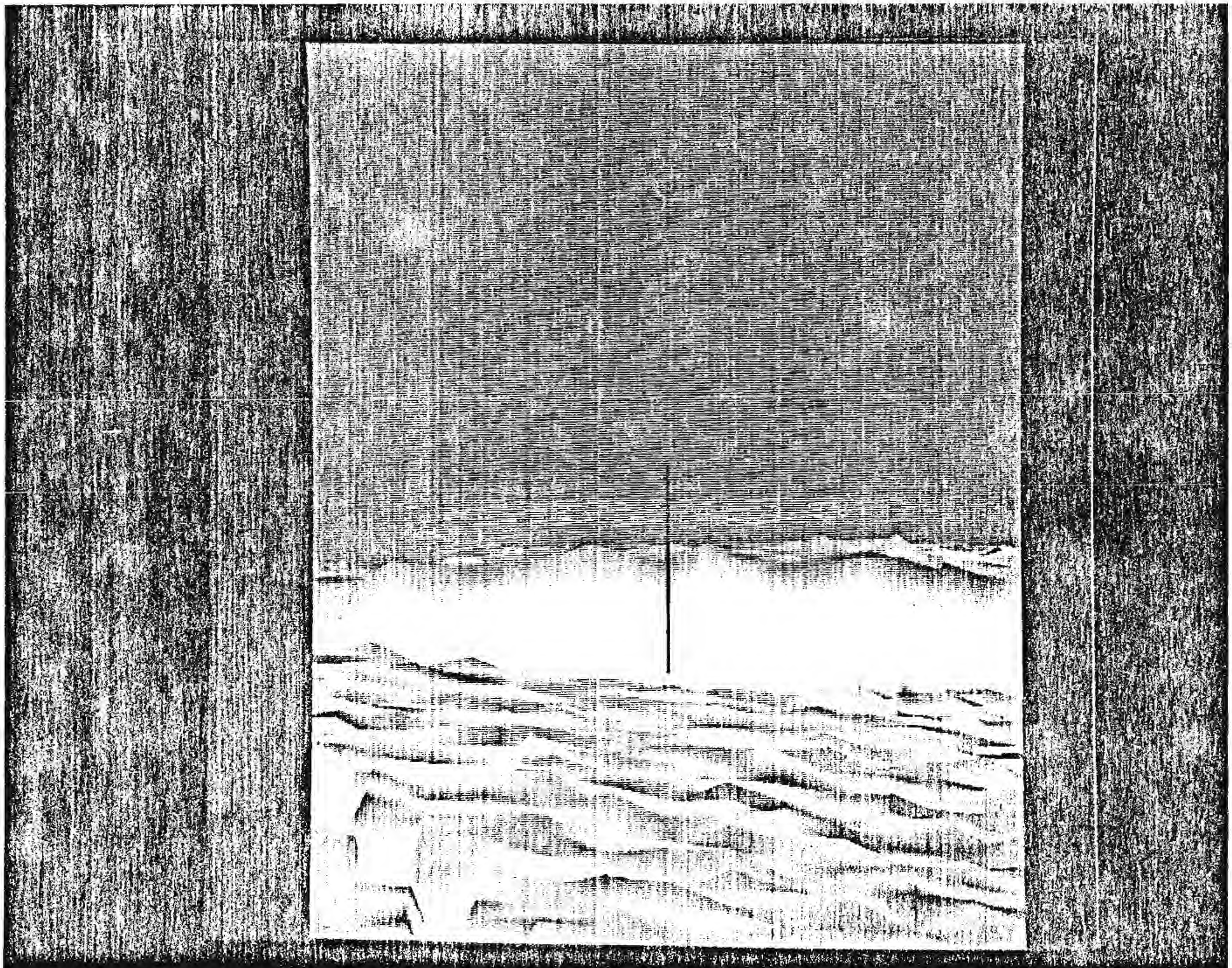

FIGURE D.3 TOWER CLOSURE SEQUENCE - 2.0 KILOMETERS

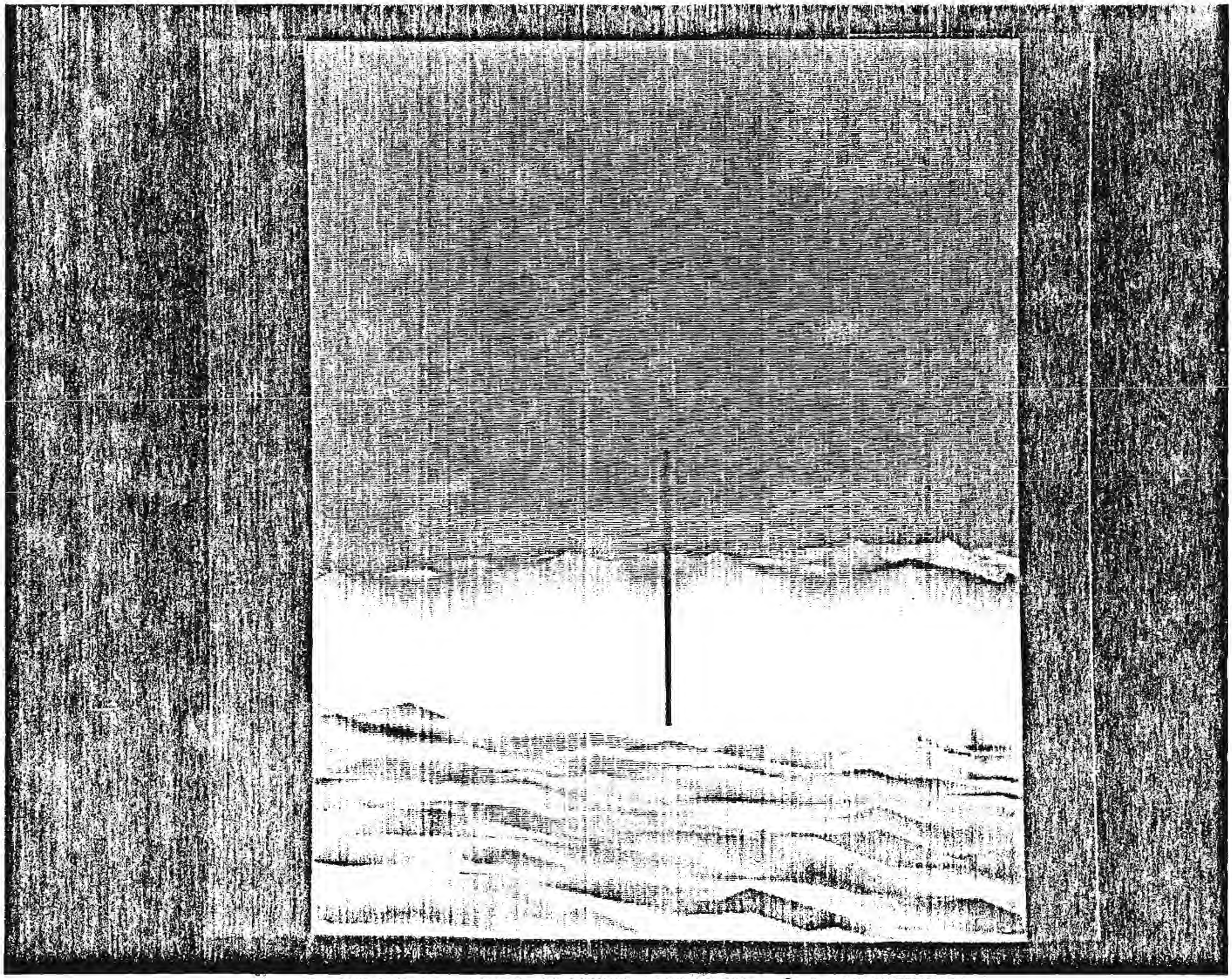

FIGURE D.4 TOWER CLOSURE SEQUENCE - 1.5 KILOMETERS

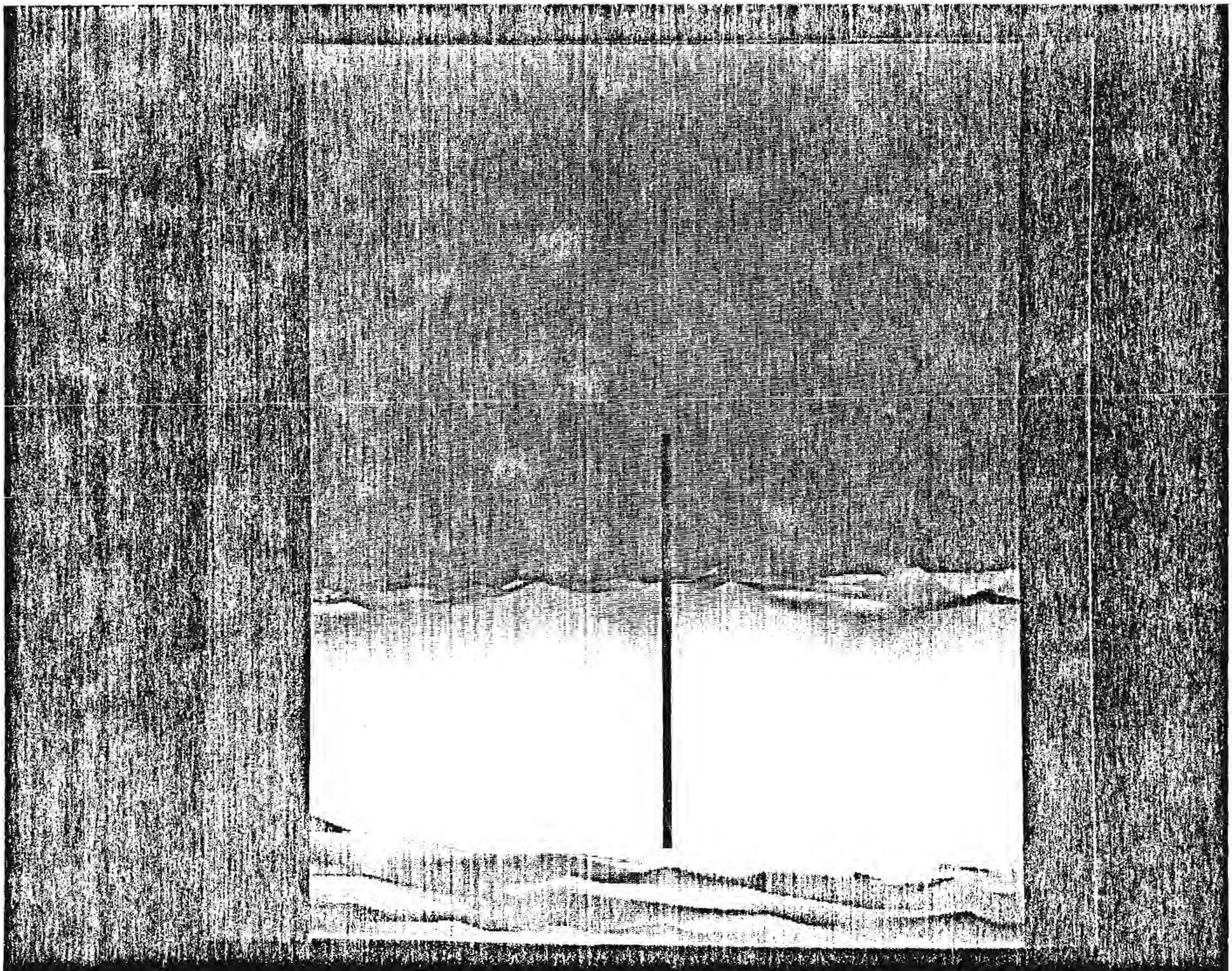

FIGURE D.5 TOWER CLOSURE SEQUENCE -1.0 KILOMETERS

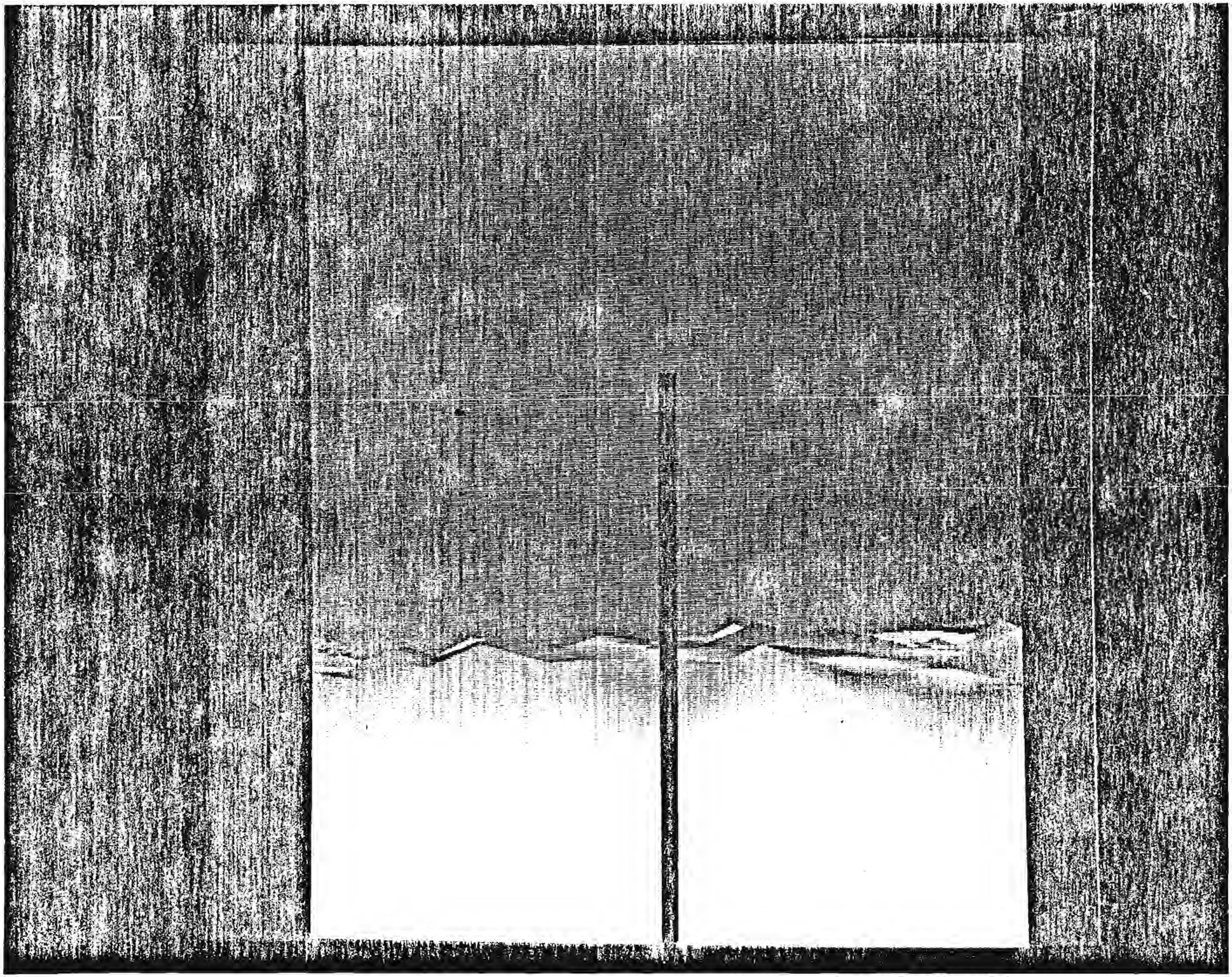

FIGURE D.6 TOWER CLOSURE SEQUENCE - 0.5 KILOMETERS